

Dynamic Plastid Redox Signals Integrate Gene Expression and Metabolism to Induce Distinct Metabolic States in Photosynthetic Acclimation in *Arabidopsis* ^W

Katharina Bräutigam,^a Lars Dietzel,^a Tatjana Kleine,^b Elke Ströher,^c Dennis Wormuth,^c Karl-Josef Dietz,^c Dörte Radke,^{d,e} Markus Wirtz,^f Rüdiger Hell,^f Peter Dörmann,^g Adriano Nunes-Nesi,^g Nicolas Schauer,^g Alisdair R. Fernie,^g Sandra N. Oliver,^g Peter Geigenberger,^{g,h} Dario Leister,^b and Thomas Pfannschmidt^{a,1}

^aNachwuchsgruppe Pflanzliche Anpassung an Umweltveränderungen: Proteinanalyse mittels MS, Lehrstuhl für Pflanzenphysiologie, Institut für Allgemeine Botanik und Pflanzenphysiologie, Friedrich-Schiller-Universität Jena, 07743 Jena, Germany

^bLehrstuhl für Botanik, Department Biologie I, Ludwig-Maximilians-Universität, 82152 Martinsried, Germany

^cLehrstuhl für Biochemie und Pflanzenphysiologie, Universität Bielefeld, 33615 Bielefeld, Germany

^dHans Knöll Institute, 07745 Jena, Germany

^eInstitute for Community Medicine, Ernst Moritz Arndt University of Greifswald, 17475 Greifswald, Germany

^fHeidelberg Institute of Plant Sciences, University of Heidelberg, 69120 Heidelberg, Germany

^gMax-Planck-Institut für Molekulare Pflanzenphysiologie, 14476 Potsdam-Golm, Germany

^hDepartment Biologie I, Ludwig-Maximilians-Universität, 82152 Martinsried, Germany

Plants possess acclimation responses in which structural reconfigurations adapt the photosynthetic apparatus to fluctuating illumination. Long-term acclimation involves changes in plastid and nuclear gene expression and is controlled by redox signals from photosynthesis. The kinetics of these signals and the adjustments of energetic and metabolic demands to the changes in the photosynthetic apparatus are currently poorly understood. Using a redox signaling system that preferentially excites either photosystem I or II, we measured the time-dependent impact of redox signals on the transcriptome and metabolome of *Arabidopsis thaliana*. We observed rapid and dynamic changes in nuclear transcript accumulation resulting in differential and specific expression patterns for genes associated with photosynthesis and metabolism. Metabolite pools also exhibited dynamic changes and indicate readjustments between distinct metabolic states depending on the respective illumination. These states reflect reallocation of energy resources in a defined and reversible manner, indicating that structural changes in the photosynthetic apparatus during long-term acclimation are additionally supported at the level of metabolism. We propose that photosynthesis can act as an environmental sensor, producing retrograde redox signals that trigger two parallel adjustment loops that coordinate photosynthesis and metabolism to adapt plant primary productivity to the environment.

INTRODUCTION

In dense plant stands, such as crop fields or forests, individuals shade each other and create competition for light absorption. As a result, the incident light intensity within the stand decreases exponentially (Terashima et al., 2005). Furthermore, selective light absorption by the upper leaf layers leads to an enrichment of far-red wavelengths that activates phytochrome-mediated shade avoidance responses (Smith, 2000). Perhaps more importantly, the light gradient additionally largely reduces the efficiency of photosynthesis. Photosystem II (PSII) and photosystem I (PSI) work electrochemically in series; however, the reaction centers differ in their absorption properties and use light quanta of

wavelengths 680 and 700 nm, respectively. The increase in far-red light induces excitation imbalances between the two photosystems that disturb both the redox chemistry in the transport chain and its coordination with the Calvin-Benson cycle, the function of which is crucial for CO₂ fixation and the recovery of the electron end acceptor NADP⁺ (Allen, 2002; Dietzel et al., 2008). Plants possess molecular acclimation mechanisms that restore the photosynthetic homeostasis by structural reconfiguration of the photosynthetic apparatus involving changes in antenna composition (state transition) and photosystem stoichiometry (long-term response [LTR]) (Aro and Andersson, 2001; Walters, 2005; Eberhard et al., 2008). These processes are relatively well characterized at the biophysical level, but the integration of gene expression and metabolism during light quality acclimation is currently poorly understood. Recent data indicate that the redox states of plastoquinone (PQ) and of thioredoxin are central to the regulation of light acclimation responses (Pfannschmidt, 2003; Schurmann, 2003; Buchanan and Balmer, 2005; Kanervo et al., 2005) and that these responses occur in a photoreceptor-independent manner (Walters et al., 1999; Fey et al., 2005).

¹ Address correspondence to thomas.pfannschmidt@uni-jena.de.

The author responsible for distribution of materials integral to the findings presented in this article in accordance with the policy described in the Instructions for Authors (www.plantcell.org) is: Thomas Pfannschmidt (thomas.pfannschmidt@uni-jena.de).

^WOnline version contains Web-only data.

www.plantcell.org/cgi/doi/10.1105/tpc.108.062018

Plastoquinone is a mobile membrane-intrinsic electron carrier that connects PSII with the cytochrome *b₆f* complex and is involved in both linear and cyclic electron transport (Allen, 2003). Therefore, it is an ideal sensor for any alteration in the electron flux through the transport chain. Thioredoxin is a small ubiquitous redox-active protein that is photosynthetically reduced by ferredoxin, which in turn acquires its electrons from the photosynthesis electron end acceptor NADPH. It exists in several subtypes and activates many chloroplast enzymes (e.g., enzymes of the Calvin-Benson cycle) via reduction of thiol groups. By this means, it is responsible for light activation of many plastid biosynthesis pathways and functional coupling of light and dark reactions of photosynthesis (Schurmann, 2003; Buchanan and Balmer, 2005; Schurmann and Buchanan, 2008). The redox states of both components depend directly on the photosynthetic electron flux and must therefore act as parallel signals that both affect photosynthetic acclimation at the same time (Fey et al., 2005; Piippo et al., 2006; Adamiec et al., 2008). Our understanding of redox regulation of plant light acclimation is further complicated since various stress-induced reactive oxygen species (ROS), such as H₂O₂ or singlet oxygen (Apel and Hirt, 2004; Mittler et al., 2004), and ROS scavenging molecules, such as glutathione, ascorbate, or peroxiredoxins, contribute to the intracellular redox signaling network (Dietz, 2003; Foyer and Noctor, 2005; Mullineaux and Rausch, 2005).

A recently identified key regulator of photosynthetic acclimation is the thylakoid-associated kinase state transition 7 (STN7), which is essential for short-term acclimation (i.e., state transitions; Bellafiore et al., 2005), and long-term acclimation (i.e., photosystem stoichiometry adjustment; Bonardi et al., 2005). Both acclimation responses are controlled by the redox state of PQ involving targeted phosphorylation of the light-harvesting complex of PSII (LHCII) and transcription changes in chloroplast and nuclear photosynthesis genes (Pfannschmidt, 2003). It is important to note that *in vitro* LHCII phosphorylation was found to be activated by a reduced PQ pool but to be inactivated by a reduced thioredoxin pool (Rintamäki et al., 2000; Hou et al., 2002). This strongly suggests that the activity of STN7 is controlled by both redox systems in a hierarchical manner (Rochaix, 2007).

Photosynthetic redox signals are widely accepted as a novel and important class of retrograde plastid signals from vital chloroplasts that coordinate expression of photosynthesis genes in both organelle and nucleus, in addition to signals from tetrapyrrole biosynthesis and signals from plastid gene expression (Nott et al., 2006; Bräutigam et al., 2007; Pesaresi et al., 2007). To study photosynthetic redox control of gene expression, different approaches using mutants, inhibitors, or varying illumination have been used (Pfannschmidt et al., 2009). Physiological systems that induce redox signals by generating excitation imbalances between the photosystems were found to be especially useful. Low-intensity excitation with artificial light sources that preferentially excite PSI or PSII (PSI or PSII light, respectively) induce either oxidation or reduction of the photosynthetic electron transport chain without induction of stress-related responses and provide an experimental system that can be used for a wide range of organisms, including cyanobacteria, algae, and plants (Melis and Harvey, 1981; Deng et al., 1989; Chow

et al., 1990; Melis et al., 1996; Pfannschmidt et al., 1999; Alfonso et al., 2000; Kovacs et al., 2000; Tullberg et al., 2000; Fan et al., 2007). This light system mimics the natural light quality gradients of dense plant populations and induces typical acclimation responses, such as state transitions and photosystem stoichiometry adjustment. In contrast with photomorphogenic responses, photosynthetic acclimation is reversible and can be easily followed by shifting plants between PSI and PSII lights. Recent studies demonstrated that light quality-induced redox signals strongly affect gene expression, photosynthetic acclimation, and growth of *Arabidopsis thaliana* (Bellafiore et al., 2005; Bonardi et al., 2005; Fey et al., 2005; Piippo et al., 2006; Wagner et al., 2008).

In this article, we combined light quality-induced redox signaling in *Arabidopsis* with systems biology approaches to analyze how photosynthesis integrates acclimation responses at the levels of gene expression and metabolism. The data presented provide a novel understanding of how photosynthetic redox signals define the physiological framework by which plants perceive and respond to their light environment.

RESULTS

Kinetics of Retrograde Redox Signals

The redox state of the photosynthetic electron transport chain in *Arabidopsis* was manipulated by growing plants under either PSI or PSII light (Fey et al., 2005; Wagner et al., 2008). Plants acclimated to these lights were shifted to the alternate condition to induce either a strong reduction (PSI-II light shift) (Figure 1A) or a strong oxidation (PSII-I light shift) (Figure 1B) signal. The LTR to such shifts was followed by collecting samples prior to the shift (t 0 control) and at 0.5, 2, 8, and 48 h thereafter. Transcript profiles from these samples were obtained using an established DNA filter array with gene-specific tags (GSTs) for nuclear genes encoding chloroplast proteins that represent the preferential targets for plastid signals, including photosynthesis-associated nuclear genes (PhANGs) (Kurth et al., 2002; Fey et al., 2005). In the PSI-II shift experiment, the initial transcriptional response occurred within the first 30 min following the shift, indicating rapid transduction of chloroplast redox signals toward the nucleus (Figure 1). In the PSII-I shift experiment, the response appeared to be slower with the first genes reacting 2 h after the shift. Also, further changes in the profiles during the course of acclimation differed between the two treatments. In the PSI-II plants (Figure 1A), numbers of downregulated genes decreased and those of upregulated genes increased continuously in the 2- and 8-h time points. At 48 h, numbers of upregulated genes slightly declined again, but the number of downregulated genes displayed a large increase. By contrast, in the PSII-I plants (Figure 1B), numbers of upregulated genes slightly decreased at the 8-h time point, while the number of downregulated genes displayed a strong transient increase, which almost completely diminished after 48 h. The number of upregulated genes at this time point increased again. Profiles of the final stage of acclimation (48 h) indicated that the reduction signal mainly induced downregulation of gene expression, while the opposite occurred

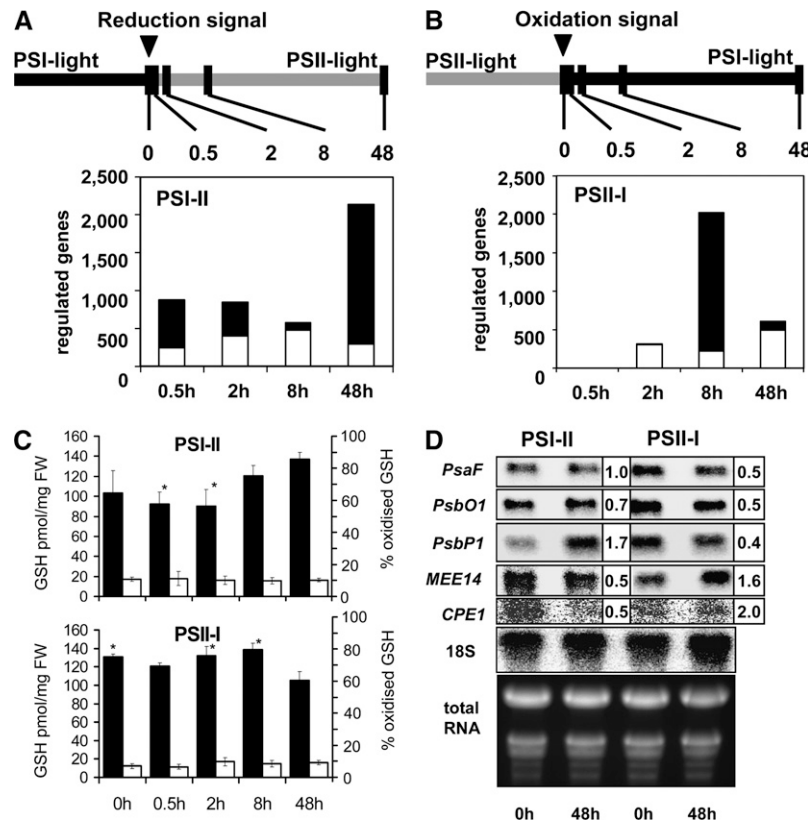


Figure 1. Experimental Setup and Expression Kinetics of Nuclear Genes for Chloroplast Proteins in Response to Redox Signals.

(A) and (B) Time courses of the PSI-II (A) and PSII-I (B) acclimation experiments are given on top, and number of regulated genes at the respective time points are given below. Marked time points indicate harvesting of material after the respective light shift. Given are numbers of genes with significant expression changes referred to the 0-h time point (t test, adjusted $P < 0.05$, $n = 4$ to 6, correction for multiple testing; Benjamini and Hochberg, 1995). White, upregulated genes; black, downregulated genes.

(C) Content and redox state of glutathione during the course of light shift experiments. Plants were grown and samples of it were obtained as described in (A) and (B). The material was used for determination of total amounts (black bars) and the proportion of oxidized (white bars) glutathione. The respective light shift is indicated. Asterisks indicate significant different mean compared with the 48-h time point ($n = 3$, SD; Bonferroni test, $P < 0.05$).

(D) Validation of macroarray expression data by RNA gel blot analysis. Selected genes with different expression behavior were tested for their accumulation at the 0- and 48-h time points (left and right lanes of each panel). Hybridization signals were detected using a phosphor imager. Relative expression changes in the arrays are given beside the respective signal.

in response to an oxidation signal. Functional analyses indicated that many genes regulated differed between the two experiments. Thus, the two acclimation responses are not merely mirrors of one another that oppositely regulate the same set of genes but represent different response programs.

Although the light sources used here represent a low-light system that does not generate direct light stress on photosynthesis (Fey et al., 2005), it cannot be excluded that sudden changes between PSI and PSII light maybe provoke the formation of ROS due to changes in electron flux. To test potential interaction and/or overlap of photosynthetic redox signals with effects of ROS in the short term, we determined glutathione amounts and its redox states at the same time points as the kinetic array analysis (Figure 1C). In both light shift experiments, no significant changes in total glutathione contents were observed at the beginning of the response. A slight increase was found at end point of the PSI-II light shift, while the opposite was observed at the end of the PSII-I light shift. The redox state of

glutathione was highly reduced under both light sources, and no apparent changes in it were detected at any time point after the shifts to the respective other light source. This excludes generation of relevant amounts of ROS even after a PSI-II light shift, which causes a sudden reduction of the transport chain.

To corroborate the findings in our array experiment, we performed independent expression analyses of a few genes using RNA gel blot analyses (Figure 1D). Five genes were chosen that exemplarily demonstrate how differential the expression behavior of genes was after the light shifts. In detail, we analyzed the photosynthesis genes *PsaF* (encoding a subunit of PSI) and *PsbO1* (encoding the 33-kD protein of the water splitting complex of PSII), which displayed no marked changes after application of a reduction signal but a clear decrease after an oxidation signal. Furthermore, we used the photosynthesis gene *PsbP1* (encoding another component of the water splitting complex), which exhibit an increase after the reduction signal and a decrease after the oxidation signal. The opposite expression

signature was observed for two metabolism genes, *MEE14* (for maternal effect embryo arrest 14) and *CPE1* (for cysteine protease inhibitor-related protein). The gene expression changes observed in the RNA gel blot analyses were comparable to the expression changes in the array analysis (see fold expression changes given in Figure 1D) and confirm the validity of the results of this experiment. This is in line with earlier reports demonstrating the reproducibility of gene expression changes found using this array (Kubis et al., 2004).

Expression Patterns of Functionally Related Gene Groups and Primary Regulated Genes

PhANGs are known to be preferential targets of retrograde plastid signals; however, in most studies, just a few representative genes, such as *Lhcb1*, *RbcS*, or *PetE* (encoding the chlorophyll binding protein 1 of the LHCII, the small subunit of ribulose-1,5-bisphosphate carboxylase/oxygenase, and plastocyanin) were tested (Susek et al., 1993; Pfannschmidt et al., 2001; Ruckle et al., 2007). Here, we analyzed the expression behavior of the whole functional group during the time course of the kinetic

and compared it to other groups of functionally related genes encoding components for carbohydrate, amino acid, and other metabolism. To this end, the expression data were imported into the Mapman software (Thimm et al., 2004; Usadel et al., 2005), and gene expression changes within functional groups were visualized (see Supplemental Figure 1 online). The expression behavior of such groups was then determined by averaging expression changes of all genes within a given functional group or bin (see Supplemental Figure 1 online) at each time point (Figure 2A) (mean expression change). In response to a reduction signal, PhANGs displayed only very weak reaction with a slight tendency to decrease after 30 min and a clear repression after 2 h (Figure 2A). After 8 h, the repression diminished and at 48 h up- and downregulated genes achieved an almost neutral balance exhibiting just a slight decrease with respect to the zero time point. In response to the oxidation signal, a completely different pattern was observed. After 30 min, PhANGs exhibited weak changes with a slight tendency to decrease, while after 2 h, increased expression in comparison to the zero time point was observed. After 8 h, the expression started to decline, and at 48 h, PhANGs were clearly repressed, displaying a continuously

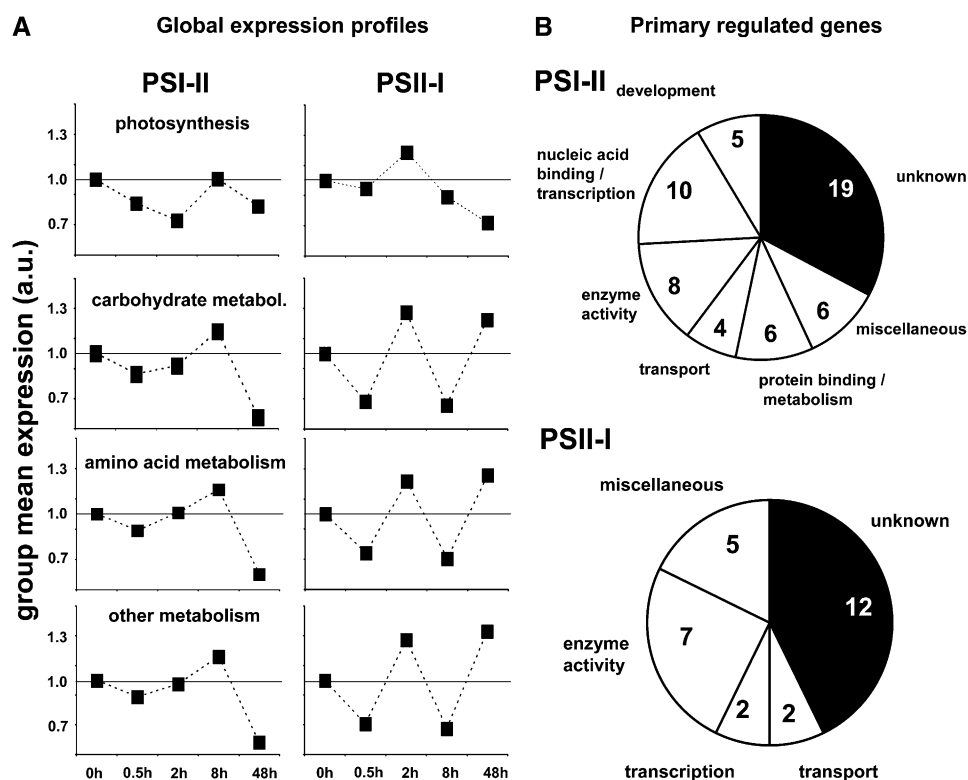


Figure 2. Dynamics of Gene Expression Changes in Response to Redox Signals.

(A) Expression kinetics of functional groups of genes. The array data were imported into the MapMan software, and expression changes in comparison to the 0 time point were visualized (see Supplemental Figure 1 online). Expression changes of all genes in one functional group according to the classification of Biehl et al. (2005) (photosynthesis, carbohydrate metabolism, amino acid metabolism, or residual metabolism) were calculated, averaged, and given as mean expression value, which reflects the reactions of the complete functional group during the course of the kinetic experiment.

(B) PRGs. Genes regulated 2.5-fold at the 30-min time point after a reduction signal (58 genes) and 2 h after an oxidation signal (28 genes) were assigned to nucleic acid binding/transcription, protein binding/metabolic function, enzymatic activity, development, transport, miscellaneous, or unknown (pie chart). For gene identity and detailed functional classification, see Supplemental Data Set 1 online.

increasing repression during the experiment. Genes for carbohydrate metabolism, including sugar and starch metabolism, revealed different expression patterns (Figure 2A). These profiles displayed a weak reaction in response to a reduction signal after 30 min with a tendency to decline. After 2 h, a neutral expression balance was achieved and a slight increase after 8 h. After 48 h, a strong general decrease was observed. In response to the oxidation signal, we observed first similar expression changes as to the reduction signal with a general decrease after 30 min, followed by an increase after 2 h. Then, a strong downregulation occurred after 8 h followed again by clear upregulation at the 48-h time point. The same expression profiles were observed for amino acid and all other functional metabolic groups (Figure 2A). Thus, at the final stages of the two experiments, the transcript profiles opposed one another. In PSI-II plants, metabolism genes are mainly downregulated, while in PSII-I plants, these genes appear to be mainly upregulated. By contrast, PhANGs are clearly downregulated in PSII-I, while in PSI-II plants, they appear to reach a more balanced expression level. We found this expression behavior significantly different from all other functional groups of genes (see Supplemental Table 1 online), indicating a specific regulation of this gene group by photosynthetic redox signals. Thus, retrograde redox signaling regulates PhANG expression in a specific way but also that of genes for other major functional groups with a special emphasis on those associated with metabolism.

The expression profiles suggest early, middle, and late responsive genes, implying a cascade of regulatory events that may affect expression of many genes by indirect means. We assumed that genes directly regulated by photosynthetic redox signals would respond quick and clearly. To identify such primary regulated genes (PRGs), we investigated the first reacting genes (after 30 min and 2 h, respectively) for those that exhibited at least 2.5-fold up- or downregulation. Fifty-eight genes from the PSI-II and 29 from the PSII-I experiment met this criterion (Figure 2B; see Supplemental Data Set 1 online). We found that PRGs do not comprise one distinct functional gene group but cover several groups. Regulated genes identified in the both experiments, however, mainly encode components with regulatory functions, including several transcription factors and protein interaction or modification factors that may initiate the regulation of secondary and tertiary target genes. Thus, photosynthetic redox regulation of nuclear genes for plastid proteins appears to be a very complex network process rather than a direct pathway. To get deeper insights into this regulation, we tried to identify regulatory elements in front of the PRGs. We analyzed the potential promoter regions of the genes to test if some common regulatory *cis*-elements exist and found a number of known promoter elements mainly involved in light regulation and development (see Supplemental Table 2 online). However, we did not find a common component that could serve as a potential redox-responsive element. This might suggest that redox signals may affect upstream components of the cellular signaling network of plants and interact with other light signaling pathways as has been suggested earlier for other plastid signals (Kusnetsov et al., 1996; Ruckle et al., 2007). To test this, PRGs were analyzed for characteristic expression signatures of other light-dependent physiological influences, such as ROS-induced expression

changes or phytochrome-mediated responses by comparison to profiles housed in various publicly available databases (see Supplemental Figure 2 online). Only very little overlap was observed between the PRGs defined here and the gene expression signatures from other experiments, indicating that the responses described here are distinct from those induced by ROS or other light signaling pathways. Thus, the expression patterns observed here are unique to photosynthetic redox signals. To confirm the dominant nature of redox signals in our light shift experiment, we performed an additional array experiment in which we compared the response of the wild type to a reduction signal after 30 min with the respective response in the *stn7* mutant (see Supplemental Figure 3 online). Due to the lack of the STN7 kinase, this mutant is expected not to respond to the reduction signal from the PQ pool; thus, redox-controlled genes in the nucleus should not display any significant expression changes. In the wild type, 937 genes were found to be significantly regulated 30 min after the reduction signal. Eight hundred of them showed no reaction in the *stn7* mutant, indicating that the great majority (85%) of the genes responding to the light shift is under redox control and that other light-dependent signaling mechanisms play a minor role in this experimental setup.

Influences of LTR on Plant Primary Photosynthates

The observed regulation of PhANG expression can be easily explained with the reorganization of the photosynthetic apparatus during the LTR; however, there is no obvious reason for the extensive regulation of metabolism genes. Given that transcriptional changes do not always correspond with those observed at the functional level (Gibon et al., 2006), we next tested whether the impact on metabolic genes was reflected in the metabolic states of plants at the end of acclimation (corresponding to the 48-h time point in the kinetic experiments). PSI and PSII-I plants showed 40 to 50% reduction in starch accumulation when compared with PSII and PSI-II plants (Figure 3A), whereas total protein and fatty acid accumulation as well as specific fatty acids remained constant (Figures 3B and 3C; see Supplemental Figure 4 and Supplemental Table 3 online). Thus, light quality acclimation appears to influence the major intermediate energy storage component of leaves and starch, while the metabolism of chloroplast lipids and proteins remains unaltered. Nevertheless, the cellular energy state (indicated by ATP/ADP ratio) was found to be relatively constant in all plants (with values varying between 0.5 and 0.8 [Figure 3D] in comparison to 2.2 in white light-grown plants [Wormuth et al., 2006]). Our data therefore suggest a low but stable energy status of the plants irrespective of the growth light regimes we applied. Calculation of the redox state of the NADP pool indicated a high NADPH/NADP⁺ ratio in PSI- or PSII-I plants and a low one in PSI-II and PSII plants, respectively (Figure 3E). In fact, that reported in PSI light was of similar magnitude to that only reported previously for plants grown under electron transport reducing conditions (~100 μ E white light) (Wormuth et al., 2006). To obtain additional experimental data on the NADP redox state, we determined the activation state of the NADP-dependent malate dehydrogenase (MDH), which serves as a proxy for the coupled redox states of the NADP and thioredoxin pools (Figure 3F). This revealed that the MDH activation state

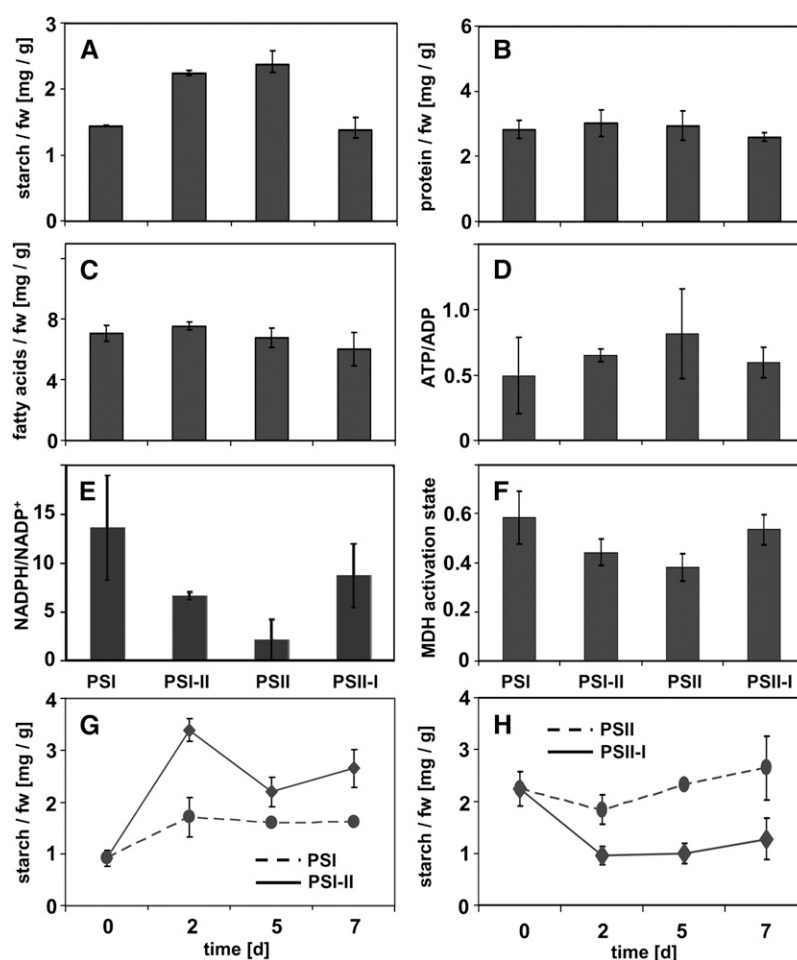


Figure 3. Primary Photosynthate Parameters.

(A) to (F) *Arabidopsis* plants were acclimated to the four standard growth programs, and basic metabolites were determined at the end of the acclimation response. Starch (A), protein (B), fatty acids (C), ATP/ADP ratio (D), NADPH/NADP⁺ ratio (E), and activation state of NADP-dependent MDH (F).

(G) and (H) Time course of changes in starch accumulation after indicated light shift. fw, fresh weight. Data represent means \pm SD ($n = 3$ to 4). See Methods for details.

was significantly higher in PSI than in PSII plants, suggesting that under PSI light, the NADP/thioredoxin system indeed might be more reduced than under PSII light. Shifting plants to the respective other light source reversed this situation.

In time-course experiments, we observed that changes in starch accumulation increased upon a PSI-II light shift within the first 2 d, followed by a decrease reaching a stable level at days 4 and 6, which was significantly higher than before the shift. By contrast, starch amounts decreased within the first 2 d after a PSII-I light shift (Figures 3G and 3H). Thereafter, the starch level remained constant, indicating that an equilibrium has been reached after the respective light quality acclimation. The changes in starch levels occurred within the same time frame in that reconstruction of the photosynthetic apparatus during the LTR occurs (Pfannschmidt et al., 2001). This suggests that the LTR stabilizes the energy state of the plants under continuous PSI or PSII light by redirecting storage energy.

LTR Induces Two Distinct Metabolic States

To further investigate this apparent differential energy resource allocation, we performed metabolic profiling 48 h after the light shifts. We focused on amino acids, sugars, and several precursor molecules for important catabolic and anabolic pathways (see Supplemental Table 4 online). A cluster analysis of all metabolite data collected indicates that a number of important organic acids (e.g., glycerate, pyruvate, and shikimate) and several amino acids that are precursor metabolites of secondary metabolism (e.g., Trp or Phe) (Figure 4A, bars 1 and 2) are coregulated. The same is true for most sugars and sugar alcohols (Figure 4A, bar 3). The cluster analysis demonstrates that PSI and PSII-I plants were similar in their metabolite content, as were the PSII and PSI-II plants. In a principal component analysis, plants acclimated to PSII light, PSI light, or white light each exhibited different metabolic states and shifts between the light sources

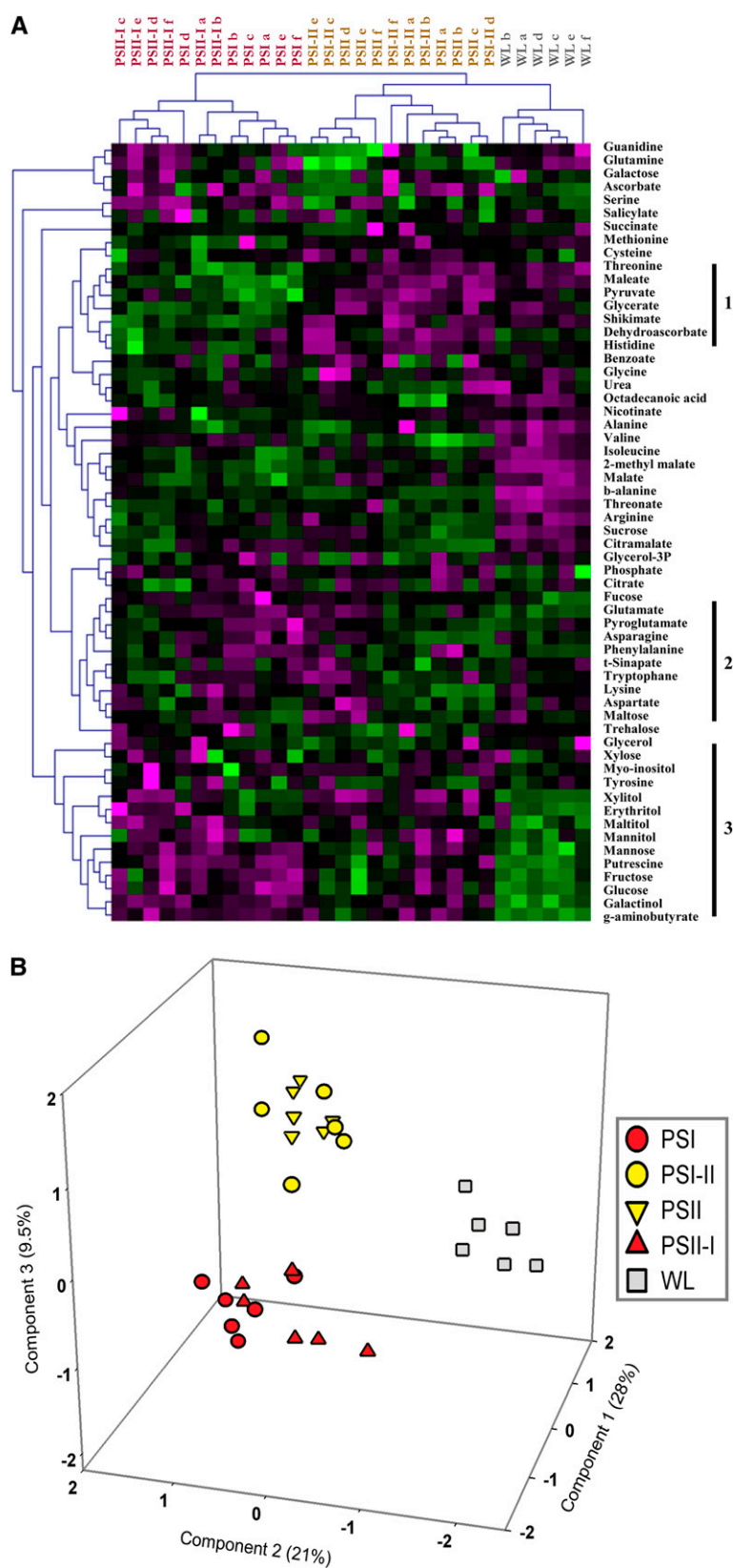


Figure 4. Metabolic Profiling.

readjusted the metabolic profiles in such a way that PSI-II plants are more similarly to PSII plants than to PSI plants (Figure 4B). The opposite reaction was found for the PSII-I plants, which showed far greater resemblance to PSI than to PSII plants. This indicates that the LTR directs the metabolism into distinct states in a reversible manner that correlates well to the transcriptional responses of genes associated with metabolism described above.

For an overview, the relative changes of metabolite levels were plotted within the context of a metabolic scheme (Figure 5). This data projection clearly revealed four different groups of metabolites based on their relative changes upon light quality shifts. The largest group represents metabolites that remain stable in their pool size regardless of the light treatment. Most importantly, this includes sucrose, the principal transport carbohydrate. The second group is comprised of metabolites that are oppositely regulated in the two light conditions. Interestingly, all compounds upregulated after a PSI-II light shift were found to be downregulated after a PSII-I light shift. This includes important organic acids, such as glycerate, shikimate, and pyruvate and the two amino acids Thr and His, but no sugars. Only one component, Gln, was upregulated after a PSII-I light shift and downregulated after a PSI-II light shift. Together with His, it forms an oppositely regulated pair of metabolites. The third group is a number of metabolites that were downregulated in the PSI-II plants but that remained stable in PSII-I plants, including several sugars and two amino acids. In the fourth group are metabolites that exhibited stable pools in PSI-II plants but that were downregulated in PSII-I plants, including some amino acids and malate. In summary, a PSI-II shift resulted in a decrease in primary products of photosynthesis, such as sugars, but an increase in important intermediates of subsequent metabolic pathways. By contrast, a PSII-I shift has no effect on the sugar pools but leads to general downregulation of many subsequent metabolites, including amino acids and organic acids. Stabilization of sugar pools in PSII-I plants is most likely achieved by the redirection of storage energy (e.g., from starch) into other metabolic pathways, resulting in a stable levels of soluble energy equivalents. In PSI-II plants, sugar contents are reduced, but a stable energetic state of the cell is achieved by an increase in many other metabolites. Thus, the LTR induces two distinct metabolic states with characteristic differences, which we designate here as metabolic state 1, corresponding to PSI light-acclimated plants, and metabolic state 2, corresponding to PSII light-acclimated plants.

Transition Kinetics between Metabolic States 1 and 2

To learn more about this metabolic reprogramming, we performed light shift experiments with plants as in our array experiments and determined changes in the amounts of selected

metabolites along the time course of acclimation (Figure 6). These experiments uncovered that many metabolite pool sizes were established in a discontinuous manner, exhibiting transient changes that were not reflected by the end point analyses. The most prominent example of this is sucrose, which was found to be stable upon shifts between metabolic states 1 and 2. In the PSI-II light shift, the sucrose amounts displayed a transient peak with a rapid increase after 30 min and 2 h and a decrease to the original level after 8 and 48 h. By contrast, in a PSII-I light shift, sucrose remained fairly constant under all conditions with a slight tendency to decline at 48 h. Gln displayed general downregulation in the PSI-II light shift and upregulation in the PSII-I light shift, however, with a transient increase at the 2-h time point in the PSI-II shift experiment. For Thr, we observed opposite trends with a slight increase in the PSI-II light shift and a slight decrease in the PSII-I light shift. As in the case of sucrose, we found a transient peak at 30 min and 2 h, which diminished after 8 h, but this time in the PSII-I shift experiment. Met revealed almost stable pool sizes in the PSI-II light shift with a slightly increased plateau at 30 min and 2 and 8 h and a tendency to decrease in the PSII-I light shift. However, all changes were very small. Glycerate exhibited a clear increase in the PSI-II light shift and a small decrease in the PSII-I shift experiment. However, the latter experiment revealed a transient increase as well as a subsequent decrease. Malate remained stable in the PSI-II light shift but exhibited a transient increase as sucrose. In the PSII-I light shift, the metabolite decreased but exhibited also a transient increase at the 30 min and 2 h time point. In summary, each of the selected metabolites exhibited a different accumulation profile for establishing the final pool size, indicating high complexity by which the two metabolic states were achieved. Another important conclusion from these experiments is that most metabolites require the full time range of the LTR to establish a novel equilibrium that is similar to the changes in the gene expression profiles. Obviously, the cellular networks require a considerable time range to fully respond to the sudden light shifts. The dynamic changes observed in both time course experiments exacerbate conclusions on causal relationships in the responses, but it is interesting to note that the transient increase in sucrose correlates in time with a transient decrease of the photosynthesis genes in the PSI-II light shift.

Physiological Consequences of the Metabolic States

Our observation of metabolic reprogramming produces a number of predictions that should be testable experimentally. One of these is that the resource allocation from starch into other metabolite pools should become limiting for plant growth under conditions when starch becomes essential as energy source (e.g., in the dark). Usually, plants in our light regimes are

Figure 4. (continued).

Metabolites were determined in six samples (a to f) per light regime (PSI, PSI-II, PSII, PSII-I, and white light).

(A) Hierarchical cluster analysis. Dendrograms summarize relatedness of metabolites (right) and samples (top). The heat map reflects increased (magenta) or decreased metabolite levels (green) with respect to the row and column mean. Bars indicate coregulated metabolites.

(B) Principal component analysis. Given principal components cover 59% of total variance in the data set. Percentage of variance explained by each component is given. Each data point represents an independent sample. Red, metabolic state 1; yellow, metabolic state 2; gray, metabolic state in white light.

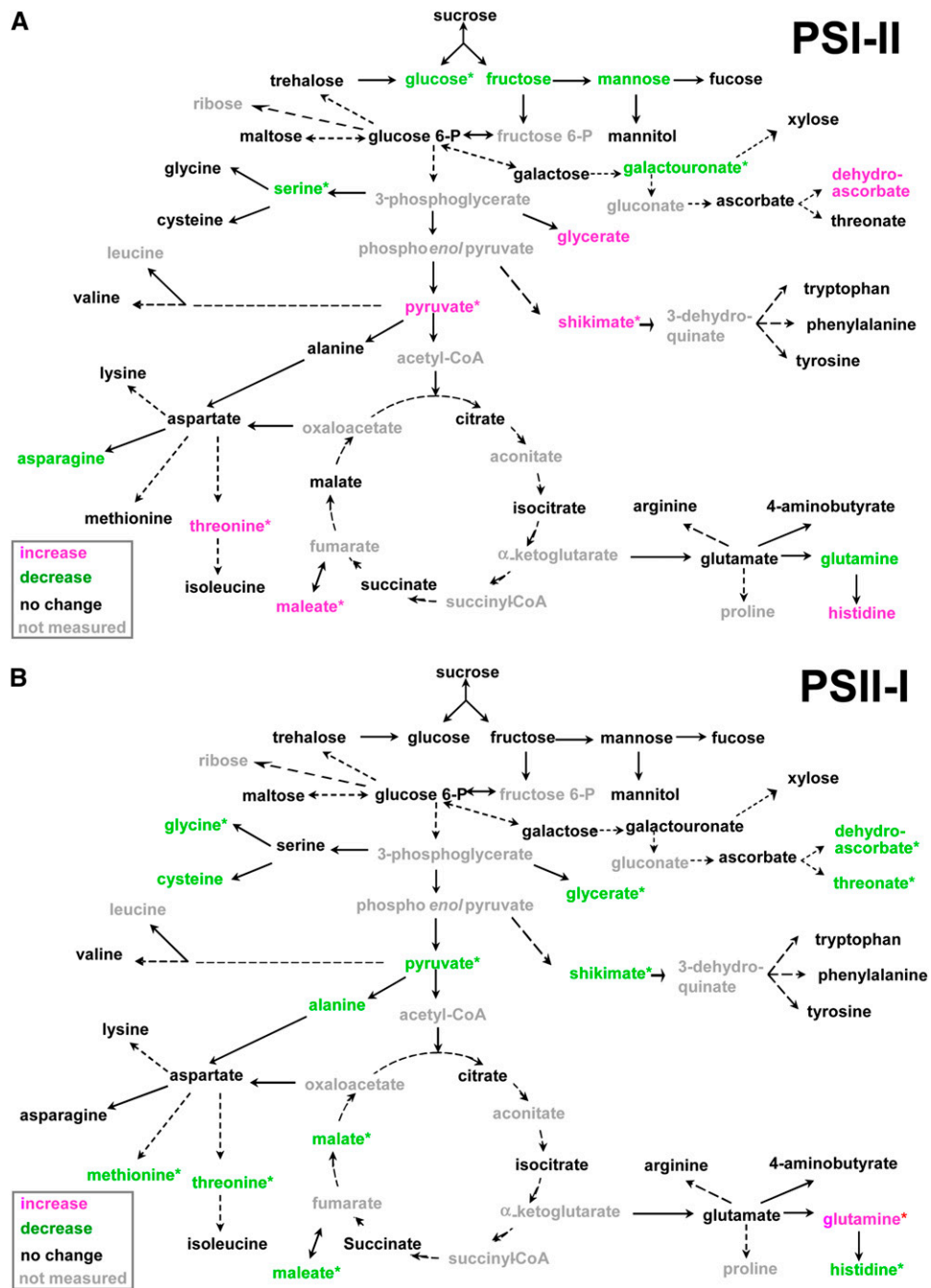


Figure 5. Metabolic States of Plants Shifted from PSI to PSII light (PSI-II, Metabolic State 2) and Vice Versa (PSII-I, Metabolic State 1).

The scheme contains central metabolic pathways of sugar and amino acid metabolism as well as the citric acid cycle (Kolbe et al., 2006). Statistical differences in metabolite accumulation after the given light shifts were calculated (Student's *t* test, $P \leq 0.05$, $n = 4$ to 6) and indicated by color code (red, increase; green, decrease). Gray, not measured; black, no significant difference. Asterisks indicate metabolites with significant changes after employing a correction for multiple testing (Benjamini and Hochberg, 1995).

illuminated 24 h per day to damp circadian rhythms. Under these conditions, *Arabidopsis* plants do not exhibit differences in rosette growth and seed production, demonstrating that the LTR is very effective in counterbalancing of the light gradients (Wagner et al., 2008). To test if the metabolic reprogramming can

induce a phenotype, plants were grown under PSI and PSII light with dark periods of increasing length. This changes the time relation of starch production to starch consumption and increases the demand for starch as energy source in plant growth (Figure 7A). In addition, we compared the response of the wild

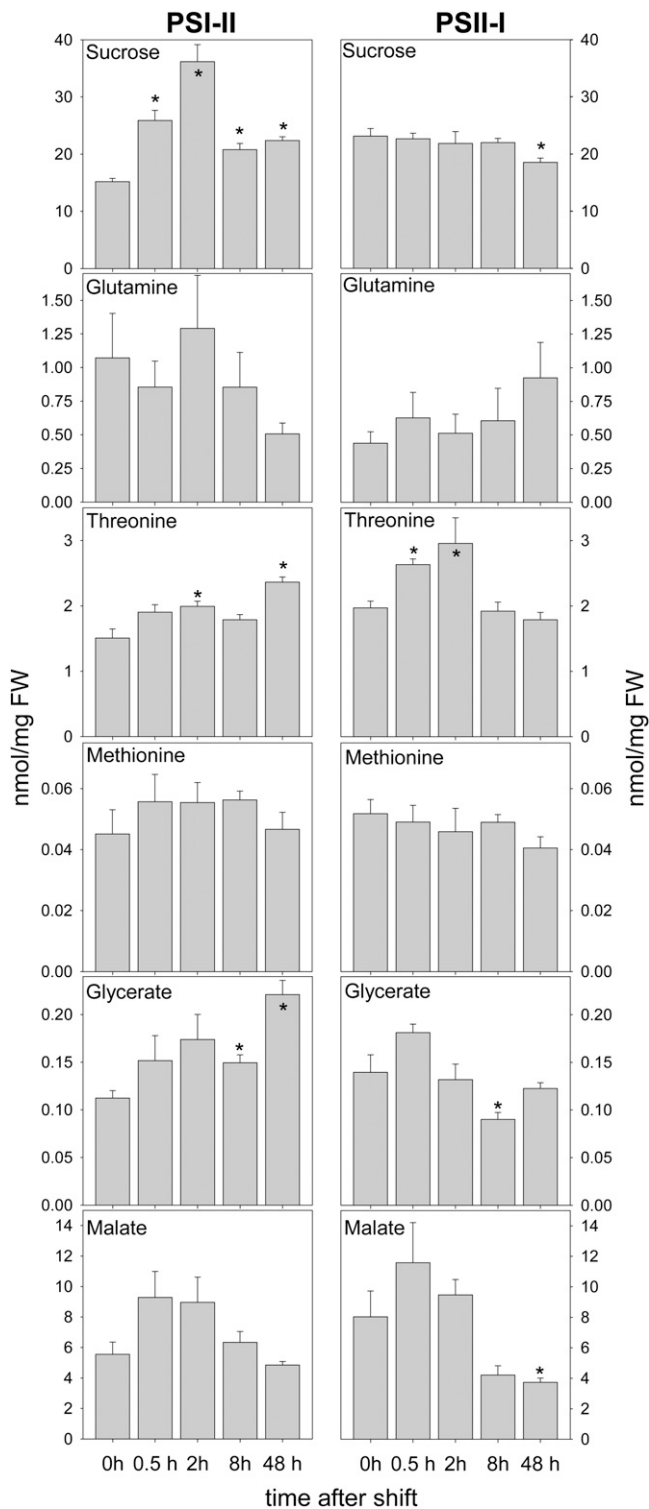


Figure 6. Kinetics of Metabolite Changes in Response to Redox Signals. Plants were grown and samples obtained as described in Figure 4. Values for metabolite levels under the different light regimes represent mean and SE of five independent measurements. Asterisks indicate significantly different mean compared with the respective 0 time point (Student's *t* test, $P \leq 0.05$, $n = 5$).

type and the mutant *stn7*, which is deficient both in state transitions and LTR due to the lack of the thylakoid-bound kinase STN7 (Bellafiore et al., 2005; Bonardi et al., 2005). A short night (8 h dark) gave no visible differences in growth; however, a long night (16 h dark) resulted in severe growth retardation under PSI light, both for the wild type and the *stn7* mutant (Figure 7A). Thus, the lower accumulation of starch in PSI light becomes limiting for growth under these conditions. Furthermore, the *stn7* mutant exhibited additional growth retardation in both conditions in comparison to the wild type. The effect under PSII light can be best explained by the lack of input of reduction signals from the PQ pool on the signaling network underlying photosynthetic acclimation since the central transducer, STN7, is absent. Determination of starch in the *stn7* mutant revealed that under PSII light this storage metabolite accumulates only to the level of PSI plants (Figure 7B). This observation is entirely consistent with similar sizes of wild-type PSI plants and *stn7* PSII plants (Figure 7A). By contrast, under PSI light the PQ pool is largely oxidized and the STN7 kinase is inactive (Wagner et al., 2008); thus, its deficiency cannot cause the additional retardation effect observed here. To a large extent, starch metabolism depends on the thioredoxin redox state and its effects on the controlling enzymes of starch synthesis (Geigenberger et al., 2005). We therefore determined the MDH activation state in the *stn7* mutant (Figure 7B). We could not observe the same differences as in the wild type but found a deregulation with an activation state lying in average between that of wild-type PSI and PSII plants. This indicates that the redox state of the thioredoxin system is stable regardless of illumination condition. Thus, an adjustment of metabolism to metabolic state 1 might be repressed in the *stn7* mutant by an inability in adapting thioredoxin redox state to the respective light condition.

DISCUSSION

Photosynthetic Redox Signaling Is Very Dynamic

Recent studies investigating the impact of photosynthetic redox signals on nuclear gene expression were performed at single distinct time points, resulting in static views of regulation patterns (Fey et al., 2005; Piippo et al., 2006; Adamiec et al., 2008). In recent studies the monitoring of changes in chlorophyll a/b ratios and reporter gene expression in transgenic tobacco (*Nicotiana tabacum*) in our light system displayed the first significant changes after 3 to 12 h (Schutze et al., 2008; Wagner et al., 2008), suggesting that gene expression changes might occur faster. So far, no very early time points have been investigated. Our kinetic array analysis includes such time points and demonstrates that transcriptional responses in the nucleus to photosynthetic redox signals are very dynamic and rapid, resembling the time range observed for the transduction of redox signals within chloroplasts (Pfannschmidt et al., 1999). This suggests that the signals are most likely transduced by preexisting pathways or mechanisms. However, the reaction to an oxidation signal appeared to be slower than to a reduction signal that is consistent with earlier observation at the physiological level where we found similar differential kinetics in changes of the

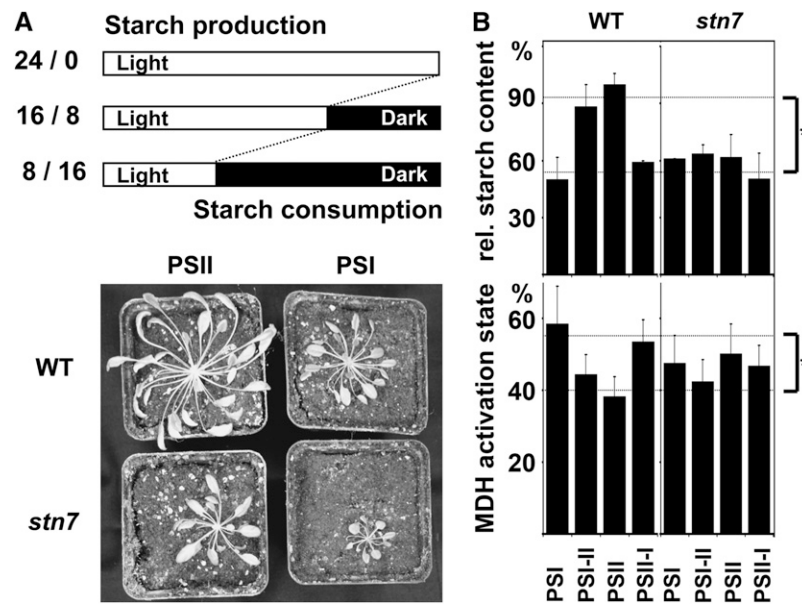


Figure 7. Physiological Consequences of Metabolite Reprogramming.

(A) Starch requirement for plant growth was forced by changing the relation of starch production (Light) to starch consumption (Dark) periods in a 24-h period (indicated by white and black bars on top of the figure). The wild type and *stn7* mutants were grown in parallel on soil. After 3 weeks of precultivation in white light on soil, plants were set in either PSI or PSII light for 15 weeks with an 8-h night (16/8) or an 8-h day (8/16). Controls received 24 h of light (24/0). Representative examples after growth in 8/16 are shown.

(B) Starch accumulation and MDH activation state in the *stn7* mutant after growth in continuous light. Data represent means \pm SD ($n = 3$). Starch accumulation of the wild type under PSII light was set as 100%. Asterisks indicate that the mean values for starch and MDH activation state of PSI and PSII-I wild-type plants were found to be significant different from that of PSII and PSI-II plants (Student's *t* test, $P \leq 0.05$, $n = 6$).

chlorophyll fluorescence parameter F_s/F_m (Wagner et al., 2008). This suggests that these signals are mediated via different pathways, which would also explain the different response programs activated in the two experiments. Another important conclusion from our kinetic experiment is that the observed impact on nuclear gene expression depends not only on the signaling system activated but also on the time point of observation and argues for further kinetic analyses also under other environmental conditions, such as light intensity or temperature shifts.

The dynamic changes in the expression profiles during the course of the response suggest a step-by-step cascade of regulation events in which redox signals regulate PRGs that activate further downstream regulation events. This is of particular interest for the assumed predominant target genes for photosynthetic redox signals, PhANGs. In our study, only a few PhANGs exhibited significant changes in transcript accumulation at early time points. However, a clear impact on the whole functional group became visible during the further course of the responses, resulting in distinct differences to each other at the end of the LTR as well as to metabolism genes during the whole course of the kinetic. Recently, GOLDEN2-LIKE transcription factors were reported to coordinate the expression of photosynthesis genes and therefore represent interesting candidates as LTR regulators (Waters et al., 2009). However, such factors were not among the identified PRGs, but a high number of other transcription factors. Interestingly, we also identified SIG1, a plastid-localized transcription initiation factor of the plastid-

encoded RNA polymerase. Its ortholog in rice (*Oryza sativa*) was reported to be of importance for the regulation of plastid-encoded photosynthesis genes (Tozawa et al., 2007). Besides transcription, it is likely that early redox signals act in parallel at other levels of regulation that have an impact on the functional group of photosynthesis genes and were not addressed here, such as posttranscriptional or translational regulation. Existence of such mechanisms has been shown earlier (Petraček et al., 1997, 1998; Sherameti et al., 2002; Frigerio et al., 2007). Unraveling the details of this regulation network and the relation to other signal transduction networks, such as those for photoreceptors or other plastid signals, will be a challenging field for future research. The expression signatures in the array analyses, however, display only very small overlap with already known transcript profiles in response to other environmental signals. Thus, the response programs to reduction and oxidation signals appear to be distinct and unique, pointing to a high independence from other signaling networks. This conclusion is further confirmed by the additional array experiments with the *stn7* mutant, in which 85% of all genes reacting to a reduction signal from the PQ pool in the wild type do not exhibit any expression change.

Metabolic Changes Contribute to LTR

So far, the LTR has been regarded as a mechanism that solely affects the structure of the photosynthetic apparatus to improve light use. Our study indicates that the LTR, in addition, involves

directed metabolic adjustments, indicating that photosynthesis has direct regulatory impact on metabolite pool sizes. This is in line with a recent report demonstrating that light intensity shifts also result in metabolic reprogramming (Frenkel et al., 2009). Thus, our data explain long-term light quality acclimation as a combinatorial readjustment of photosystem stoichiometry and metabolic activity by the combined impact of photosynthetic redox control on gene expression and enzyme networks. This integrates redox control of energy metabolism into the context of acclimation. Interestingly, state transitions in *Chlamydomonas reinhardtii* have been explained as a similar mechanism shifting the unicellular alga between two extreme metabolic states, ATP generation by cyclic electron transport or linear electron transport (Wollman, 2001). State transitions in this unicellular alga are much more pronounced than in higher plants, an effect which is probably due to the requirement that a unicellular organism needs to respond much more drastically to environmental changes because of its limited resources. It appears that the major role of state transitions in *Chlamydomonas* is to reach ATP homeostasis. Here, we also observed relatively stable ATP/ADP ratios, however, at a very low level that is far below known values for white light-grown plants (Figure 4D; Wormuth et al., 2006). Our metabolite profiling also confirms that metabolic states 1 and 2 are different from that in white light-grown plants (Figure 4B), suggesting that this is a specific strategy to redistribute metabolic energy under light-limited conditions. These data also demonstrate that, like *Chlamydomonas*, higher plants can shift between distinct metabolic states in a reversible way that is much more sophisticated than a simple on-off switch by light-dark transitions. Furthermore, these metabolic states are obviously adapted to the respective functional state of photosynthesis under the two illumination conditions. Our growth experiment with increasing dark periods resulted in conditional phenotypes that made this resource allocation visible, indicating that these two metabolic states do possess direct relevance for plant growth performance. The enhanced phenotypes of the *stn7* mutant, in addition, clearly demonstrate that the metabolic reprogramming is not functional after genetic suppression of the LTR, indicating that it is really controlled by photosynthetic redox signals. It could be argued that the observed resource allocation is simply caused by the lack of state transitions in the *stn7* mutant; however, the physiological setup of the growth experiments does exclude this possibility. At the end of the dark period, plants are in state 1 and a shift into PSII light then induces a state 2 transition, which does not take place in the *stn7* mutant. However, the enhanced phenotype of the mutant occurs only with a 16-h dark period but not with an 8-h dark period, indicating that a long-term process rather than the lack of the state transition is the decisive parameter for the phenotype. This is supported by the experiment when plants are shifted from the dark into PSI light. Here, the plants remain in state 1 and no state transitions occur at all; however, the mutant still exhibited an enhanced phenotype, indicating that the suppression of the LTR is the reason for the observed growth differences. These observations demonstrate that photosynthesis has a strong impact on plant development and also support the notion that redox signaling networks seem to act largely independently from other light signaling networks, such as those controlled by photoreceptors. This is in line with our conclusion from the comparison of expression signatures in PRGs and

photoreceptor-controlled genes (see Supplemental Figure 2 online) as well as from the results of our additional array experiment (see Supplemental Figure 3 online).

Two Adjustment Loops Constitute Long-Term Light Quality Acclimation

Based on our data, we propose an extended model for the establishment of LTR (Figure 8). Any imbalance in excitation energy distribution caused by environmental changes generates changes in the redox states of electron transport components or coupled redox mediators (i.e., PQ and thioredoxin), which serve as signals that regulate two parallel adjustment loops. In the photosynthetic adjustment loop, expression of photosynthesis

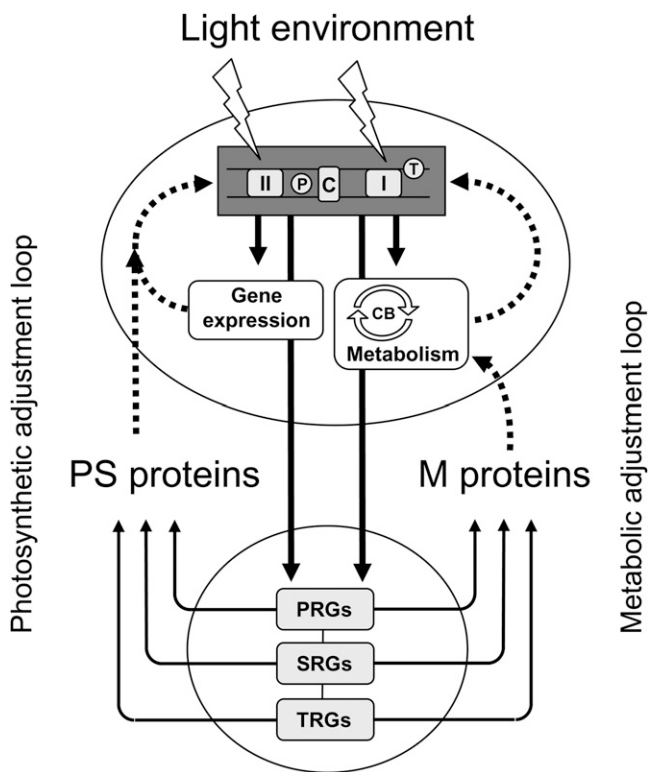


Figure 8. Model of Photosynthetic and Metabolic Adjustment Loops during Photosynthetic Long-Term Acclimation.

Chloroplast and nucleus compartments are shown as an oval and circle, respectively. The photosynthetic electron transport chain is drawn schematically as a dark-gray sensor box perceiving the environmental light (P, plastoquinone pool; C, cytochrome *b₆f* complex; T, thioredoxin pool). Light-induced redox signals originating from this sensor box (black arrows) affect plastid gene expression and metabolism (the white arrow circle represents the Calvin-Benson [CB] cycle). In parallel, redox signals are transmitted to the nucleus where they affect a cascade of primary, secondary, and tertiary regulated genes (PRGs, SRGs, and TRGs), which lead to changes in corresponding photosynthesis (PS) and metabolism (M) proteins. These are transported into the plastid where they contribute to formation of novel components of the photosynthetic electron transport chain or changes in enzyme pools of the metabolism.

genes is affected, resulting in changes of amounts of proteins for the photosynthesis apparatus. These support a structural reconfiguration of the whole apparatus, which optimizes light harvesting and utilization under the respective environmental condition. In the metabolic adjustment, loop redox signals affect metabolic processes within the plastids (and most probably also in the cytosol) and the expression of metabolism genes in the nucleus. This leads to changes in the accumulation of metabolic enzymes, resulting in changes of metabolite fluxes and the establishment of different metabolic states. These states, in turn, are adapted to the efficiency of photosynthetic function and the production of primary photosynthates required for metabolic reactions. By this means, photosynthesis serves as a sensor box for plants that integrates various environmental influences, such as light, temperature, or CO₂ availability, and adjusts its own structure and metabolite pools accordingly. Both adjustment loops consist of an inner and an outer loop. The inner loop is located within the plastid and involves the well-known redox regulation of plastid gene expression and photosynthetic dark reaction (see Introduction). The outer loop extends to the cytosol and nucleus and affects photosynthesis and metabolism genes in distinct patterns (cf. Figure 2) by a sequential activation or repression of primary, secondary, and tertiary genes. The expression changes finally lead to changes of corresponding proteins that are imported into the plastid. The inner regulation loop provides a means for integration of these cytosolic proteins into plastid functions in a plastid-autonomous and specific way that satisfies the demands of the single plastid. By contrast, the outer loop reflects the general demands of the whole cell since it reflects the integration of the redox signals from all plastids. Our kinetic experiments both at the levels of gene expression and metabolite pools indicate that these loops require a considerable amount of time (i.e., days to establish a novel equilibrium after a change in the environment). In this context, photosynthetic short-term acclimation, such as state transitions or nonphotochemical quenching, may serve as buffering systems that minimize or damp quick oscillations of redox signals created in the photosynthetic apparatus by the highly fluctuating environment. Such damping systems lead to a stabilization of the metabolic fluxes and hence optimize plant primary production. This is in agreement with recent reports studying the function of such short-term responses (Tikkanen et al., 2006; Frenkel et al., 2007, 2009). The tight functional linking between the photosynthetic and metabolic adjustment loops suggests that any disturbance in one of the (inner or outer) loops will have an impact on the others by feedback mechanisms. This can be observed in many mutants, for example, with defects in photosynthesis that display changes in metabolites or in metabolism mutants that display changes in photosynthesis (Walters et al., 2003, 2004; Hausler et al., 2009).

Coordination of Photosynthesis, Gene Expression, and Metabolism in the LTR

Our model provides a mechanistic idea for a very precise fine-tuning of gene expression and metabolism in photosynthetic light acclimation; however, it is unclear how the respective illumination condition is actually sensed. An oxidized or reduced state of the PQ pool as induced by PSI or PSII light would not be

an unambiguous signal since this leads to overlaps with situations of the redox states in the dark or white light. Therefore, we assume that a second component or parameter is necessary to indicate the residing light environment. A likely candidate is the redox state of the thioredoxin pool, which seems to be also affected by the light sources. Redox signaling gradients have been proposed for thioredoxin control of enzyme activities (Schurmann and Buchanan, 2008), and it is possible that the combination of redox changes in the PQ and thioredoxin pools act as cooperative signals that coordinate gene expression and metabolism. The MDH activation state suggests a more oxidized redox state of thioredoxin in PSII than in PSI light, which contrasts the general expectation and conclusions from a comparable study (Piippo et al., 2006). On the other hand, this would provide additional degrees of freedom in generation of photosynthetic redox signals by means of a binary redox control mode in which pairs of redox states from PQ and thioredoxin generate distinct signals that would be sufficient to represent a number of different illumination conditions. Determining if this binary redox control mode is really functional requires further experimental confirmation, including direct determination of thioredoxin redox states. However, cooperative redox signaling is not an unknown phenomenon since it has been proposed earlier to regulate translation initiation of the *psbA* gene in *Chlamydomonas*, activity of the LHClI kinase, and chloroplast gene expression in plants (Rintamaki et al., 2000; Trebitsh et al., 2000; Trebitsh and Danon, 2001; Hou et al., 2002; Pfannschmidt and Liere, 2005; Rochaix, 2007; Lemeille et al., 2009; Steiner et al., 2009).

Two other questions arise from our experiments: (1) what is the physiological function of the metabolic adjustment, and (2) how are the redox signals transmitted from the chloroplast to the nucleus? In PSII-I plants, many sugars remained stable, while many other metabolite pools, including starch, decreased in their size, which is consistent with the activation of many enzymes by a more reduced thioredoxin system and the increased expression of many metabolism genes. In PSI-II plants, a number of sugar pools were downregulated, while many metabolites and starch were upregulated. This is consistent with a decrease in metabolism gene expression and downregulation of enzyme activities via a more oxidized thioredoxin system. Most importantly, sucrose remained stable under both conditions. It is conceivable that this stabilization is the major goal of the metabolic shifts observed here. Resource allocation between metabolite pools thus could provide a buffering system generating sucrose homeostasis in the plant under varying and different illumination conditions. However, the kinetic experiments with selected metabolites clearly indicated that the novel metabolic states are established dynamically with highly variable accumulation patterns. Most importantly in the context of cellular energy resources was the observation that in the PSI-II light shift experiment a transient sucrose peak occurs in which sucrose increased from 15 to 35 $\mu\text{mol/g}$ fresh weight (corresponding to an increase from ~ 15 to 35 mM if it is assumed that sucrose is equally distributed within the cell). High concentrations of sucrose have been reported to repress photosynthesis gene expression and to induce genes of storage metabolism (Rook et al., 2006). This is precisely what can be found in the expression patterns of the array kinetic and suggests an interaction of redox

signals with the sugar signaling network. Interaction of redox and sugar signals in regulation of photosynthesis gene expression has been reported earlier, however, in a different physiological system, namely, *Arabidopsis* cell suspension cultures (Oswald et al., 2001). The increase in sucrose correlates with an increase in starch levels (Figure 3G), and it is conceivable to assume that the surplus of sucrose is used to synthesize this storage compound, which in turn would explain the transient nature of the sucrose peak. Thus, can it be concluded that the redox signal is converted into a sugar signal? At this stage of knowledge, this cannot be finally answered; however, it appears unlikely since in the PSII-I light shift, no changes in sucrose concentrations occur at all, but photosynthesis genes are downregulated, pointing to sucrose-independent regulation of the gene group in the light system. This suggests that the transient sucrose peak following the PSI-II light shift may merely be the result of downregulation of sucrose consumption, which is then counterbalanced by increased starch synthesis. On the other hand, the *stn7* mutant does not show any increase in starch upon a PSI-II light shift most probably since it is unable to transmit the right redox signals. It was shown that an interaction of redox and sugar signals is required for regulation of starch synthesis, suggesting that both must be active at the same time rather than working in a sequential manner (Kolbe et al., 2005; Michalska et al., 2009). Unraveling the precise interactions in this regulation will be a major task of future research. However, maintaining the transport carbohydrate sucrose at a constant level provides a good explanation for the equal seed production of *Arabidopsis* grown under PSI and PSII light as observed earlier (Wagner et al., 2008).

In summary, our study indicates that in plants, a complex photosynthetic control performs fine-tuning not only of photosynthesis but also of metabolic reactions especially under light-limiting conditions. Retrograde redox signals therefore represent an integral part of the cellular signaling system playing an essential role under physiological conditions and demonstrating the importance of the concept of operational control of plastids (Pogson et al., 2008). This fine-tuning is essential for efficient energy conversion and maximum plant fitness pointing to an important target for plant yield improvements in dense plant populations, such as crop fields or forests, where strong light gradients persist.

METHODS

Growth Conditions and Plant Material

Arabidopsis thaliana wild-type (Columbia) and *stn7* mutant plants were grown on soil and acclimated to PSI or PSII light as described earlier (Fey et al., 2005; Wagner et al., 2008). White light control plants were grown at $\sim 35 \mu\text{mol photons m}^{-2} \text{ s}^{-1}$ PAR. The original seeds for *stn7* T-DNA insertion mutants were kindly provided by the SALK Institute. For kinetic experiments, plants preacclimated to either PSI or PSII light were shifted to the respective other light source and samples were taken at indicated time points. Harvested material was frozen in liquid nitrogen directly in the growth cabinets and stored at -80°C until further use.

RNA Preparations

Total RNA for array and RNA gel blot analyses was isolated using the TRIzol reagent (Invitrogen) as described earlier (Fey et al., 2005). Con-

centration and purity of RNA samples were determined spectroscopically in a Biophotometer (Eppendorf). Intactness was proven by ethidium bromide staining of rRNA species after electrophoretic separation of aliquots on denaturing 1.2% agarose gels containing formaldehyde. Isolated RNA was stored at -80°C until further use.

Transcript Profiling in the Kinetic Experiment

A nylon filter DNA array carrying 3292 GSTs (including 2661 nuclear genes for chloroplast proteins and 631 genes coding for nonchloroplast proteins) was used to test the impact of light-induced redox signals on their expression. This filter array was successfully used before to test 101 different conditions or mutants (Richly et al., 2003; Biehl et al., 2005). PSI-II and PSII-I experiments were done separately in neighboring growth cabinets of the same climate chamber. Plants were acclimated to either PSI or PSII light and then shifted to the respective other light. Three independent samples were harvested at each indicated time point for RNA preparation. Total RNA was isolated from at least 200 to 500 individual plants per sample. Three independent hybridization experiments for each time point with different filters and independent radioactively labeled cDNA probes were performed, thus minimizing variation between individual plants, filters, and probes. For cDNA synthesis, 25 to 30 μg of each RNA preparation was primed with an oligonucleotide mixture matching the 3292 genes in antisense orientation, followed by a synthesis and labeling reaction including $[\alpha\text{-}^{32}\text{P}]\text{dCTP}$. These probes were hybridized to the GST filter array as described before (Kurth et al., 2002; Richly et al., 2003). Images were read with a Storm PhosphorImager (Molecular Dynamics). Using the software ArrayVision 6.0 (Imaging Research), the signal intensity of each cDNA spot on the array was quantified. The normalized artifact removed volume (*nARVOL*) was used to quantify expression abundance. In total, four to six *nARVOL* values were acquired for each gene per sample. A *t* test with false discovery rate correction (Benjamini and Hochberg, 1995) implemented in the MIDAW tool (Romualdi et al., 2005) was performed to identify statistically significant differential expression values (adjusted *P* values < 0.05). Reproducibility of the expression data with this GST filter array has been demonstrated earlier (Kubis et al., 2004; Biehl et al., 2005). Data were deposited at the Gene Expression Omnibus database (<http://www.ncbi.nlm.nih.gov/geo/>), and the accession of the transcript profiles is GSE9235. MIAME is given.

For the detection of redox-controlled genes using the *stn7* mutant as control, wild-type and mutant plants were grown as in the PSI-II array experiment. Plant material was harvested 30 min after the light shift under the light sources and frozen in liquid nitrogen, and RNA was prepared in triplicates as described above. Expression data were obtained from a commercial service as Affymetrix GeneChip data generated with Affymetrix GeneChip Operating 1.4 and Expression Console 1.1 Software using the ATH1 full-genome array. For comparison with the expression data from the GST array, only the 3292 genes were used for analysis.

Expression Data Analysis

For detailed analysis, time points 30 min after a PSI-II light shift and 2 h after a PSII-I light shift were chosen. Genes significantly regulated with a factor ≥ 2.5 were selected as potential primary targets and assigned to one of six major categories: nucleic acid binding/transcription, protein binding/metabolic function, enzymatic activity, development, transport, miscellaneous, or unknown. A more detailed functional classification was inferred from electronic annotation according to TAIR9 (see Supplemental Data Set 1 online). Average expression ratios derived from three independent experiments were analyzed by *k*-means clustering using TigrMev3.02 software (Saeed et al., 2003). To visualize the overall impact of photosynthetic control during the kinetic experiments, expression data were incorporated into the Mapman software (Thimm et al., 2004; Usadel

et al., 2005), and expression changes were indicated by a color code (see Supplemental Figure 1 online).

RNA Gel Blot Analysis

RNA gel blotting and hybridization of probes were performed using standard procedures (Sambrook and Russel, 2001). Ten micrograms of total RNA were separated on debaturing 1.2% agarose gels containing formaldehyde, blotted on a nylon membrane, and hybridized with DNA probes labeled with ^{32}P -dCTP using the random prime labeling system from GE Healthcare. After washing, the filters were exposed to a phosphor imager screen and analyzed (Storm; GE Healthcare). The following primer pairs were used to generate the probes: *PsaF* (At1g31330), forward, 5'-CGAATCTCGTTCTCAACCC-3', and reverse, 5'-CTGACCCGCATAACAATCC-3'; *PsbO1* (At5g66570), forward, 5'-GTAAATGCTCCGACGCTG-3', and reverse, 5'-GTAGCATGGCACCGAGAA-3'; *PsbP1* (At1g06680), forward, 5'-CGTGTCTGCTCTCAAACC-3', and reverse, 5'-GTTGTCTTCGAACCTAAGGACTTG-3'; *MEE14* (At2g15890), forward, 5'-TTGTTCAAGCACCAGAGACG-3', and reverse, 5'-GTCAGGAGCGTGAGAGAACC-3'; *CPE1* (At2g31980), forward, 5'-GGTTTCTGGTGTCTGCTGT-3', and reverse, 5'-GCCATTGGGTTGAGTGACTT-3'; and 18S rDNA, forward, 5'-TAAGACCAGGAGCGTATC-3', and reverse, 5'-ATTCTTGTCTGCTCTCC-3'.

Detection of Expression Signatures

To assess possible influences of ROS or phytochromes (phy) in the experimental light system used here, transcript data of early regulated genes were compared with published transcript profiles to detect genes presumably regulated by ROS or phy. Six studies analyzing the effect of different ROS, such as hydrogen peroxide, superoxide anions, or singlet oxygen, were considered (Desikan et al., 2001; op den Camp et al., 2003; Rizhsky et al., 2003; Mittler et al., 2004; Davletova et al., 2005; Vanderauwera et al., 2005). Data from five experiments studying effects of phytochrome A or B were used (Kuno et al., 2000; Wang et al., 2002; Monte et al., 2004; T. Kretsch, <http://affymetrix.arabidopsis.info>). If not detailed further, parameter and data sets from the original publication were used. In Rizhsky et al. (2003) and Davletova et al. (2005), a fold change of 2 or more was considered, and genes differentially regulated in the *phy* mutant were selected (Davletova et al., 2005). In Wang et al. (2002), genes responding in four different ecotypes to far-red light and with an impaired response in the *phyA* mutant were considered. Data sets reflecting the effect of far-red light were generated by T. Kretsch within the AtGenExpress-Project/AFGN framework and were obtained as MAS5.0 files from the NASCArray platform (<http://affymetrix.arabidopsis.info>, experiment ID = 124). Data were preprocessed and analyzed using R (version 2.4.1.) and Bioconductor software (Gentleman et al., 2004). To identify differentially expressed genes, a *t* test was performed employing correction for multiple testing (Benjamini and Hochberg, 1995). Significant genes regulated with a factor of 2.0 or more were selected. When comparing red light treatment (phytochrome B influence) with the dark control (Monte et al., 2004), genes with at least twofold regulation were used for the comparison.

Glutathione Content and Redox State

Plants were acclimated to different light sources as described in growth conditions and ground in liquid nitrogen to a fine powder. Twenty-five milligrams of powder from comparable samples were used for isolation of total or oxidized thiols as described earlier (Fey et al., 2005). Derivatization of thiols with monobromobimane (Calbiochem) and separation of thiol derivatives were performed as described earlier (Wirtz et al., 2004) using the same HPLC system. Millenium32 software (Waters) was used for data acquisition and processing. All values for each time point were determined as triplicates, and the significantly different mean (\pm SD) compared with

the 48-h time point was calculated according to the Bonferoni test ($P < 0.05$).

Primary Photosynthate Parameters

Starch, proteins, and lipids were determined by standard methods (Magel, 1991). ATP, ADP, NADP reduction state, and NADP-MDH activation state were determined and calculated as described (Kaiser and Urbach, 1977; Dietz and Heber, 1986). MDH activation state has been regarded as reporter for thioredoxin redox state (Scheibe, 1990).

Metabolite Measurements by Gas Chromatography–Mass Spectroscopy

Relative metabolite content was determined as described (Roessner et al., 2001) in six separate measurements per light regime (or time point in kinetic analyses), and \log_2 -transformed data were used for further analysis. Statistical analyses of metabolomic data were performed employing SPSS 11.0 software (SPSS), R statistical software (www.r-project.org), and Microsoft Excel. Differences in metabolite content between the two light regimes were determined by a *t* test ($P < 0.05$, Benjamini-Hochberg correction for multiple testing; Benjamini and Hochberg, 1995). Dimensional reduction was performed with a principal component analysis using standardized data. Missing data were replaced by 0. Hierarchical clustering was performed with standardized metabolites and samples using euclidean distances and average linkage. The heat map was generated with TigrMev3.02 software. Web sources for statistical software are as follows: R statistical software, <http://www.r-project.org>; TigrMev software, <http://www.tm4.org/mev.html>; NASCArray, <http://affymetrix.arabidopsis.info>; and Bioconductor, <http://www.bioconductor.org>.

Accession Numbers

Data of transcript profiles were deposited at the Gene Expression Omnibus database. The accession number is GSE9235. MIAME is given.

Supplemental Data

The following materials are available in the online version of this article.

Supplemental Figure 1. Visualization of Gene Expression Changes Using the Mapman Software.

Supplemental Figure 2. Detection of Expression Signatures of ROS or Phytochrome Signaling in Early Responsive Genes.

Supplemental Figure 3. Detection of Numbers of Redox-Controlled Genes Using the *stn7* Mutant.

Supplemental Figure 4. Fatty Acid Composition in Differentially Acclimated Plants.

Supplemental Table 1. Expression of Photosynthesis Genes Compared with Other Functional Categories.

Supplemental Table 2. Overrepresented Motifs of 4–6 bp in Length within Potential Promoter Sequences of PRGs.

Supplemental Table 3. Metabolomics Data Used in Figures 4 and 5.

Supplemental Table 4. Data of Fatty Acid Determinations Used in Supplemental Figure 4.

Supplemental Data Set 1. Identity and Expression Changes of Primary Regulated Genes Described in Figure 2.

ACKNOWLEDGMENTS

Meta Brost and Nicole Manthei are acknowledged for skilful technical assistance and Juliane Heidenbluth and Doreen Köhler for support in

starch and glutathione determinations. Special thanks go to Ekkehard Neuhaus for stimulating discussions on starch metabolism. This work was supported by grants from the Deutsche Forschungsgemeinschaft to T.P., P.G., and the research groups FOR 387 and FOR 804, by the Freistaat Thüringen (Nachwuchsgruppe: Pflanzliche Anpassung an Umweltveränderungen: Proteinanalyse mittels MS) (T.P.), and by the Bundesministerium für Bildung und Forschung (T.P., D.R.).

Received July 10, 2008; revised July 22, 2009; accepted August 20, 2009; published September 8, 2009.

REFERENCES

- Adamiec, M., Drath, M., and Jackowski, G. (2008). Redox state of plastoquinone pool regulates expression of *Arabidopsis thaliana* genes in response to elevated irradiance. *Acta Biochim. Pol.* **55**: 161–174.
- Alfonso, M., Perewoska, I., and Kirilovsky, D. (2000). Redox control of psbA gene expression in the cyanobacterium *Synechocystis* PCC 6803. Involvement of the cytochrome b(6)/f complex. *Plant Physiol.* **122**: 505–515.
- Allen, J.F. (2002). Plastoquinone redox control of chloroplast thylakoid protein phosphorylation and distribution of excitation energy between photosystems: Discovery, background, implications. *Photosynth. Res.* **73**: 139–148.
- Allen, J.F. (2003). Cyclic, pseudocyclic and noncyclic photophosphorylation: New links in the chain. *Trends Plant Sci.* **8**: 15–19.
- Apel, K., and Hirt, H. (2004). Reactive oxygen species: Metabolism, oxidative stress, and signal transduction. *Annu. Rev. Plant Biol.* **55**: 373–399.
- Aro, E.-M., and Andersson, B. (2001). Regulation of Photosynthesis. (Dordrecht, The Netherlands: Kluwer Academic Publishers).
- Bellafiore, S., Bameche, F., Peltier, G., and Rochaix, J.D. (2005). State transitions and light adaptation require chloroplast thylakoid protein kinase STN7. *Nature* **433**: 892–895.
- Benjamini, Y., and Hochberg, Y. (1995). Controlling the false discovery rate - A practical and powerful approach to multiple testing. *J. Roy. Stat. Soc. B Met.* **57**: 289–300.
- Biehl, A., Richly, E., Noutsos, C., Salamini, F., and Leister, D. (2005). Analysis of 101 nuclear transcriptomes reveals 23 distinct regulons and their relationship to metabolism, chromosomal gene distribution and co-ordination of nuclear and plastid gene expression. *Gene* **344**: 33–41.
- Bonardi, V., Pesaresi, P., Becker, T., Schleiff, E., Wagner, R., Pfannschmidt, T., Jahns, P., and Leister, D. (2005). Photosystem II core phosphorylation and photosynthetic acclimation require two different protein kinases. *Nature* **437**: 1179–1182.
- Bräutigam, K., Dietzel, L., and Pfannschmidt, T. (2007). Plastid-nucleus communication: Anterograde and retrograde signalling in development and function of plastids. In *Cell and Molecular Biology of Plastids*, R. Bock, ed (Berlin: Springer), pp. 409–455.
- Buchanan, B.B., and Balmer, Y. (2005). Redox regulation: A broadening horizon. *Annu. Rev. Plant Biol.* **56**: 187–220.
- Chow, W.S., Melis, A., and Anderson, J.M. (1990). Adjustments of photosystem stoichiometry in chloroplasts improve the quantum efficiency of photosynthesis. *Proc. Natl. Acad. Sci. USA* **87**: 7502–7506.
- Davletova, S., Rizhsky, L., Liang, H., Shengqiang, Z., Oliver, D.J., Coutu, J., Shulaev, V., Schlauch, K., and Mittler, R. (2005). Cytosolic ascorbate peroxidase 1 is a central component of the reactive oxygen gene network of *Arabidopsis*. *Plant Cell* **17**: 268–281.
- Deng, X.W., Tonkyn, J.C., Peter, G.F., Thornber, J.P., and Grissem, W. (1989). Post-transcriptional control of plastid messenger-RNA accumulation during adaptation of chloroplasts to different light quality environments. *Plant Cell* **1**: 645–654.
- Desikan, R., Mackerness, S.A.H., Hancock, J.T., and Neill, S.J. (2001). Regulation of the *Arabidopsis* transcriptome by oxidative stress. *Plant Physiol.* **127**: 159–172.
- Dietz, K.J. (2003). Redox control, redox signaling, and redox homeostasis in plant cells. *Int. Rev. Cytol.* **228**: 141–193.
- Dietz, K.J., and Heber, U. (1986). Light and CO₂ limitation of photosynthesis and states of the reactions regenerating ribulose 1,5-bisphosphate or reducing 3-phosphoglycerate. *Biochim. Biophys. Acta* **848**: 392–401.
- Dietzel, L., Bräutigam, K., and Pfannschmidt, T. (2008). Photosynthetic acclimation: State transitions and adjustment of photosystem stoichiometry - functional relationships between short-term and long-term light quality acclimation in plants. *FEBS J.* **275**: 1080–1088.
- Eberhard, S., Finazzi, G., and Wollman, F.A. (2008). The dynamics of photosynthesis. *Annu. Rev. Genet.* **42**: 463–515.
- Fan, D.Y., Hope, A.B., Smith, P.J., Jia, H., Pace, R.J., Anderson, J.M., and Chow, W.S. (2007). The stoichiometry of the two photosystems in higher plants revisited. *Biochim. Biophys. Acta* **1767**: 1064–1072.
- Fey, V., Wagner, R., Bräutigam, K., Wirtz, M., Hell, R., Dietzmann, A., Leister, D., Oelmüller, R., and Pfannschmidt, T. (2005). Retrograde plastid redox signals in the expression of nuclear genes for chloroplast proteins of *Arabidopsis thaliana*. *J. Biol. Chem.* **280**: 5318–5328.
- Foyer, C.H., and Noctor, G. (2005). Redox homeostasis and antioxidant signaling: A metabolic interface between stress perception and physiological responses. *Plant Cell* **17**: 1866–1875.
- Frenkel, M., Bellafiore, S., Rochaix, J.D., and Jansson, S. (2007). Hierarchy amongst photosynthetic acclimation responses for plant fitness. *Physiol. Plant.* **129**: 455–459.
- Frenkel, M., Kulheim, C., Johansson Jankapaa, H., Skogstrom, O., Dall'osto, L., Agren, J., Bassi, R., Moritz, T., Moen, J., and Jansson, S. (2009). Improper excess light dissipation in *Arabidopsis* results in a metabolic reprogramming. *BMC Plant Biol.* **9**: 12.
- Frigerio, S., Campoli, C., Zorzan, S., Fantoni, L.I., Crosatti, C., Drepper, F., Haehnel, W., Cattivelli, L., Morosinotto, T., and Bassi, R. (2007). Photosynthetic antenna size in higher plants is controlled by the plastoquinone redox state at the post-transcriptional rather than transcriptional level. *J. Biol. Chem.* **282**: 29457–29469.
- Geigenberger, P., Kolbe, A., and Tiessen, A. (2005). Redox regulation of carbon storage and partitioning in response to light and sugars. *J. Exp. Bot.* **56**: 1469–1479.
- Gentleman, R.C., et al. (2004). Bioconductor: Open software development for computational biology and bioinformatics. *Genome Biol.* **5**: R80.
- Gibon, Y., Usadel, B., Blaessing, O.E., Kamlage, B., Hoehne, M., Trethewey, R., and Stitt, M. (2006). Integration of metabolite with transcript and enzyme activity profiling during diurnal cycles in *Arabidopsis* rosettes. *Genome Biol.* **7**: R76.
- Hausler, R.E., Geimer, S., Kunz, H.H., Schmitz, J., Dormann, P., Bell, K., Hetfeld, S., Guballa, A., and Flugge, U.I. (2009). Chlororespiration and grana hyperstacking: How an *Arabidopsis* double mutant can survive despite defects in starch biosynthesis and daily carbon export from chloroplasts. *Plant Physiol.* **149**: 515–533.
- Hou, C.X., Pursiheimo, S., Rintamäki, E., and Aro, E.M. (2002). Environmental and metabolic control of LHCII protein phosphorylation: Revealing the mechanisms for dual regulation of the LHCII kinase. *Plant Cell Environ.* **25**: 1515–1525.
- Kaiser, W., and Urbach, W. (1977). The effect of dihydroxyacetone phosphate and 3-phosphoglycerate on O₂ evolution and on the levels

- of ATP, ADP and Pi in isolated intact chloroplasts. *Biochim. Biophys. Acta* **459**: 337–346.
- Kanervo, E., Suorsa, M., and Aro, E.M.** (2005). Functional flexibility and acclimation of the thylakoid membrane. *Photochem. Photobiol. Sci.* **4**: 1072–1080.
- Kolbe, A., Oliver, S.N., Fernie, A.R., Stitt, M., van Dongen, J.T., and Geigenberger, P.** (2006). Combined transcript and metabolite profiling of *Arabidopsis* leaves reveals fundamental effects of the thiol-disulfide status on plant metabolism. *Plant Physiol.* **141**: 412–422.
- Kolbe, A., Tiessen, A., Schluepmann, H., Paul, M., Ulrich, S., and Geigenberger, P.** (2005). Trehalose-6-phosphate regulates starch synthesis via post-translational redox-activation of ADP-glucose pyrophosphorylase. *Proc. Natl. Acad. Sci. USA* **102**: 11118–11123.
- Kovacs, L., Wiessner, W., Kis, M., Nagy, F., Mende, D., and Demeter, S.** (2000). Short- and long-term redox regulation of photosynthetic light energy distribution and photosystem stoichiometry by acetate metabolism in the green alga, *Chlamydomonas reinhardtii*. *Photosynth. Res.* **65**: 231–247.
- Kubis, S., Patel, R., Combe, J., Bedard, J., Kovacheva, S., Lilley, K., Biehl, A., Leister, D., Rios, G., Koncz, C., and Jarvis, P.** (2004). Functional specialization amongst the *Arabidopsis* Toc159 family of chloroplast protein import receptors. *Plant Cell* **16**: 2059–2077.
- Kuno, N., Muramatsu, T., Hamazato, F., and Furuya, M.** (2000). Identification by large-scale screening of phytochrome-regulated genes in etiolated seedlings of *Arabidopsis* using a fluorescent differential display technique. *Plant Physiol.* **122**: 15–24.
- Kurth, J., Varotto, C., Pesaresi, P., Biehl, A., Richly, E., Salamini, F., and Leister, D.** (2002). Gene-sequence-tag expression analyses of 1,800 genes related to chloroplast functions. *Planta* **215**: 101–109.
- Kusnetsov, V., Bolle, C., Lubberstedt, T., Sopory, S., Herrmann, R. G., and Oelmüller, R.** (1996). Evidence that the plastid signal and light operate via the same cis-acting elements in the promoters of nuclear genes for plastid proteins. *Mol. Gen. Genet.* **252**: 631–639.
- Lemeille, S., Willig, A., Depege-Fargeix, N., Delessert, C., Bassi, R., and Rochaix, J.D.** (2009). Analysis of the chloroplast kinase STT7 during state transitions. *PLoS Biol.* **7**: e45.
- Magel, E.** (1991). Qualitative and quantitative determination of starch by a colorimetric method. *Starch* **43**: 384–387.
- Melis, A., and Harvey, G.W.** (1981). Regulation of photosystem stoichiometry, chlorophyll-a and chlorophyll-b content and relation to chloroplast ultrastructure. *Biochim. Biophys. Acta* **637**: 138–145.
- Melis, A., Murakami, A., Nemson, J.A., Aizawa, K., Ohki, K., and Fujita, Y.** (1996). Chromatic regulation in *Chlamydomonas reinhardtii* alters photosystem stoichiometry and improves the quantum efficiency of photosynthesis. *Photosynth. Res.* **47**: 253–265.
- Michalska, J., Zaubner, H., Buchanan, B.B., Cejudo, F.J., and Geigenberger, P.** (2009). NTRC links built-in thioredoxin to light and sucrose in the regulation of starch synthesis in chloroplasts and amyloplasts. *Proc. Natl. Acad. Sci. USA* **106**: 9908–9913.
- Mittler, R., Vonderauwera, S., Gollery, M., and Van Breusegem, F.** (2004). Reactive oxygen gene network of plants. *Trends Plant Sci.* **9**: 490–498.
- Monte, E., Tepperman, J.M., Al-Sady, B., Kaczorowski, K.A., Alonso, J.M., Ecker, J.R., Li, X., Zhang, Y.L., and Quail, P.H.** (2004). The phytochrome-interacting transcription factor, PIF3, acts early, selectively, and positively in light-induced chloroplast development. *Proc. Natl. Acad. Sci. USA* **101**: 16091–16098.
- Mullineaux, P.M., and Rausch, T.** (2005). Glutathione, photosynthesis and the redox regulation of stress-responsive gene expression. *Photosynth. Res.* **86**: 459–474.
- Nott, A., Jung, H.S., Koussevitzky, S., and Chory, J.** (2006). Plastid-to-nucleus retrograde signaling. *Annu. Rev. Plant Biol.* **57**: 739–759.
- op den Camp, R.G.L., Przybyla, D., Ochsenbein, C., Laloi, C., Kim, C.H., Danon, A., Wagner, D., Hideg, E., Gobel, C., Feussner, I., Nater, M., and Apel, K.** (2003). Rapid induction of distinct stress responses after the release of singlet oxygen in *Arabidopsis*. *Plant Cell* **15**: 2320–2332.
- Oswald, O., Martin, T., Dominy, P.J., and Graham, I.A.** (2001). Plastid redox state and sugars: Interactive regulators of nuclear-encoded photosynthetic gene expression. *Proc. Natl. Acad. Sci. USA* **98**: 2047–2052.
- Pesaresi, P., Schneider, A., Kleine, T., and Leister, D.** (2007). Interorganellar communication. *Curr. Opin. Plant Biol.* **10**: 600–606.
- Petracek, M.E., Dickey, L.F., Huber, S.C., and Thompson, W.F.** (1997). Light-regulated changes in abundance and polyribosome association of ferredoxin mRNA are dependent on photosynthesis. *Plant Cell* **9**: 2291–2300.
- Petracek, M.E., Dickey, L.F., Nguyen, T.T., Gatz, C., Sowinski, D.A., Allen, G.C., and Thompson, W.F.** (1998). Ferredoxin-1 mRNA is destabilized by changes in photosynthetic electron transport. *Proc. Natl. Acad. Sci. USA* **95**: 9009–9013.
- Pfannschmidt, T.** (2003). Chloroplast redox signals: how photosynthesis controls its own genes. *Trends Plant Sci.* **8**: 33–41.
- Pfannschmidt, T., Brautigam, K., Wagner, R., Dietzel, L., Schroter, Y., Steiner, S., and Nykytenko, A.** (2009). Potential regulation of gene expression in photosynthetic cells by redox and energy state: Approaches towards better understanding. *Ann. Bot. (Lond.)* **103**: 599–607.
- Pfannschmidt, T., and Liere, K.** (2005). Redox regulation and modification of proteins controlling chloroplast gene expression. *Antioxid. Redox Signal.* **7**: 607–618.
- Pfannschmidt, T., Nilsson, A., and Allen, J.F.** (1999). Photosynthetic control of chloroplast gene expression. *Nature* **397**: 625–628.
- Pfannschmidt, T., Schütze, K., Brost, M., and Oelmüller, R.** (2001). A novel mechanism of nuclear photosynthesis gene regulation by redox signals from the chloroplast during photosystem stoichiometry adjustment. *J. Biol. Chem.* **276**: 36125–36130.
- Piippo, M., Allahverdiyeva, Y., Paakkari, V., Suoranta, U.M., Battchikova, N., and Aro, E.M.** (2006). Chloroplast-mediated regulation of nuclear genes in *Arabidopsis thaliana* in the absence of light stress. *Physiol. Genomics* **25**: 142–152.
- Pogson, B.J., Woo, N.S., Förster, B., and Small, I.D.** (2008). Plastid signalling to the nucleus and beyond. *Trends Plant Sci.* **13**: 602–609.
- Richly, E., Dietzmann, A., Biehl, A., Kurth, J., Laloi, C., Apel, K., Salamini, F., and Leister, D.** (2003). Covariations in the nuclear chloroplast transcriptome reveal a regulatory master-switch. *EMBO Rep.* **4**: 491–498.
- Rintamäki, E., Martinsuo, P., Pursiheimo, S., and Aro, E.M.** (2000). Cooperative regulation of light-harvesting complex II phosphorylation via the plastoquinol and ferredoxin-thioredoxin system in chloroplasts. *Proc. Natl. Acad. Sci. USA* **97**: 11644–11649.
- Rizhsky, L., Liang, H., and Mittler, R.** (2003). The water-water cycle is essential for chloroplast protection in the absence of stress. *J. Biol. Chem.* **278**: 38921–38925.
- Rochaix, J.D.** (2007). Role of thylakoid protein kinases in photosynthetic acclimation. *FEBS Lett.* **581**: 2768–2775.
- Roessner, U., Luedemann, A., Brust, D., Fiehn, O., Linke, T., Willmitzer, L., and Fernie, A.R.** (2001). Metabolic profiling allows comprehensive phenotyping of genetically or environmentally modified plant systems. *Plant Cell* **13**: 11–29.
- Romualdi, C., Vitulo, N., Del Favero, M., and Lanfranchi, G.** (2005). MIDAW: A web tool for statistical analysis of microarray data. *Nucleic Acids Res.* **33**: W644–649.
- Rook, F., Hadingham, S.A., Li, Y., and Bevan, M.W.** (2006). Sugar and ABA response pathways and the control of gene expression. *Plant Cell Environ.* **29**: 426–434.
- Ruckle, M.E., DeMarco, S.M., and Larkin, R.M.** (2007). Plastid signals

- remodel light signaling networks and are essential for efficient chloroplast biogenesis in *Arabidopsis*. *Plant Cell* **19**: 3944–3960.
- Saeed, A.I., et al.** (2003). TM4: A free, open-source system for microarray data management and analysis. *Biotechniques* **34**: 374–378.
- Sambrook, J., and Russel, D.W.** (2001). *Molecular Cloning: A Laboratory Manual*. (Cold Spring Harbor, NY: Cold Spring Harbor Laboratory Press).
- Scheibe, R.** (1990). Light dark modulation - Regulation of chloroplast metabolism in a new light. *Bot. Acta* **103**: 327–334.
- Schurmann, P.** (2003). Redox signaling in the chloroplast: The ferredoxin/thioredoxin system. *Antioxid. Redox Signal.* **5**: 69–78.
- Schurmann, P., and Buchanan, B.B.** (2008). The ferredoxin/thioredoxin system of oxygenic photosynthesis. *Antioxid. Redox Signal.* **10**: 1235–1273.
- Schutze, K., Steiner, S., and Pfannschmidt, T.** (2008). Photosynthetic redox regulation of the plastocyanin promoter in tobacco. *Physiol. Plant.* **133**: 557–565.
- Sherameti, I., Nakamura, M., Yamamoto, Y.Y., Pfannschmidt, T., Obokata, J., and Oelmüller, R.** (2002). Polyribosome loading of spinach mRNAs for photosystem I subunits is controlled by photosynthetic electron transport - A crucial cis element in the spinach *PsaD* gene is located in the 5'-untranslated region. *Plant J.* **32**: 631–639.
- Smith, H.** (2000). Phytochromes and light signal perception by plants—an emerging synthesis. *Nature* **407**: 585–591.
- Steiner, S., Dietzel, L., Schröter, Y., Fey, V., Wagner, R., and Pfannschmidt, T.** (2009). The role of phosphorylation in redox regulation of photosynthesis genes *psaA* and *psbA* during photosynthetic acclimation of mustard. *Mol. Plant* **2**: 416–429.
- Susek, R.E., Ausubel, F.M., and Chory, J.** (1993). Signal-transduction mutants of *Arabidopsis* uncouple nuclear *Cab* and *RbcS* gene-expression from chloroplast development. *Cell* **74**: 787–799.
- Terashima, I., Araya, T., Miyazawa, S., Sone, K., and Yano, S.** (2005). Construction and maintenance of the optimal photosynthetic systems of the leaf, herbaceous plant and tree: An eco-developmental treatise. *Ann. Bot. (Lond.)* **95**: 507–519.
- Thimm, O., Blasing, O., Gibon, Y., Nagel, A., Meyer, S., Kruger, P., Selbig, J., Müller, L.A., Rhee, S.Y., and Stitt, M.** (2004). MAPMAN: A user-driven tool to display genomics data sets onto diagrams of metabolic pathways and other biological processes. *Plant J.* **37**: 914–939.
- Tikkanen, M., Piippo, M., Suorsa, M., Sirpio, S., Mulo, P., Vainonen, J., Vener, A.V., Allahverdiyeva, Y., and Aro, E.M.** (2006). State transitions revisited - a buffering system for dynamic low light acclimation of *Arabidopsis*. *Plant Mol. Biol.* **62**: 779–793.
- Tozawa, Y., Teraishi, M., Sasaki, T., Sonoike, K., Nishiyama, Y., Itaya, M., Miyao, A., and Hirochika, H.** (2007). The plastid sigma factor SIG1 maintains photosystem I activity via regulated expression of the *psaA* operon in rice chloroplasts. *Plant J.* **52**: 124–132.
- Trebitsh, T., and Danon, A.** (2001). Translation of chloroplast *psbA* mRNA is regulated by signals initiated by both photosystems II and I. *Proc. Natl. Acad. Sci. USA* **98**: 12289–12294.
- Trebitsh, T., Levitan, A., Sofer, A., and Danon, A.** (2000). Translation of chloroplast *psbA* mRNA is modulated in the light by counteracting oxidizing and reducing activities. *Mol. Cell. Biol.* **20**: 1116–1123.
- Tullberg, A., Alexciev, K., Pfannschmidt, T., and Allen, J.F.** (2000). Photosynthetic electron flow regulates transcription of the *psaB* gene in pea (*Pisum sativum* L.) chloroplasts through the redox state of the plastoquinone pool. *Plant Cell Physiol.* **41**: 1045–1054.
- Usadel, B., et al.** (2005). Extension of the visualization tool MapMan to allow statistical analysis of arrays, display of corresponding genes, and comparison with known responses. *Plant Physiol.* **138**: 1195–1204.
- Vanderauwera, S., Zimmermann, P., Rombauts, S., Vandenabeele, S., Langebartels, C., Gruissem, W., Inze, D., and Van Breusegem, F.** (2005). Genome-wide analysis of hydrogen peroxide-regulated gene expression in *Arabidopsis* reveals a high light-induced transcriptional cluster involved in anthocyanin biosynthesis. *Plant Physiol.* **139**: 806–821.
- Wagner, R., Dietzel, L., Bräutigam, K., Fischer, W., and Pfannschmidt, T.** (2008). The long-term response to fluctuating light quality is an important and distinct light acclimation mechanism that supports survival of *Arabidopsis thaliana* under low light conditions. *Planta* **228**: 573–587.
- Walters, R.G.** (2005). Towards an understanding of photosynthetic acclimation. *J. Exp. Bot.* **56**: 435–447.
- Walters, R.G., Ibrahim, D.G., Horton, P., and Kruger, N.J.** (2004). A mutant of *Arabidopsis* lacking the triose-phosphate/phosphate translocator reveals metabolic regulation of starch breakdown in the light. *Plant Physiol.* **135**: 891–906.
- Walters, R.G., Rogers, J.J.M., Shephard, F., and Horton, P.** (1999). Acclimation of *Arabidopsis thaliana* to the light environment: the role of photoreceptors. *Planta* **209**: 517–527.
- Walters, R.G., Shephard, F., Rogers, J.J.M., Rolfe, S.A., and Horton, P.** (2003). Identification of mutants of *Arabidopsis* defective in acclimation of photosynthesis to the light environment. *Plant Physiol.* **131**: 472–481.
- Wang, H.Y., Ma, L.G., Habashi, J., Li, J.M., Zhao, H.Y., and Deng, X.W.** (2002). Analysis of far-red light-regulated genome expression profiles of phytochrome A pathway mutants in *Arabidopsis*. *Plant J.* **32**: 723–733.
- Waters, M.T., Wang, P., Korkaric, M., Capper, R.G., Saunders, N.J., and Langdale, J.A.** (2009). GLK transcription factors coordinate expression of the photosynthetic apparatus in *Arabidopsis*. *Plant Cell* **21**: 1109–1128.
- Wirtz, M., Droux, M., and Hell, R.** (2004). O-acetylserine (thiol) lyase: an enigmatic enzyme of plant cysteine biosynthesis revisited in *Arabidopsis thaliana*. *J. Exp. Bot.* **55**: 1785–1798.
- Wollman, F.A.** (2001). State transitions reveal the dynamics and flexibility of the photosynthetic apparatus. *EMBO J.* **20**: 3623–3630.
- Wormuth, D., Baier, M., Kandlbinder, A., Scheibe, R., Hartung, W., and Dietz, K.J.** (2006). Regulation of gene expression by photosynthetic signals triggered through modified CO₂ availability. *BMC Plant Biol.* **6**: 15.